

Constructing Bitwisted Face Pairing 3-Manifolds

Robert James Ackermann

Thesis submitted to the Faculty of the
Virginia Polytechnic Institute and State University
in partial fulfillment of the requirements for the degree of

MASTER OF SCIENCE
in
Mathematics

APPROVED:

Dr. William J. Floyd
Dr. James E. Thomson
Dr. Ezra A. Brown

April 29, 2008
Blacksburg, Virginia

Keywords: Bitwisted 3-manifolds, Twisted 3-manifolds, Dehn Surgery, face pairings,
Poincaré Sphere, 3-Torus

© Robert Ackermann

Constructing Bitwisted Face Pairing 3-Manifolds

Robert Ackermann

(ABSTRACT)

The bitwist construction, originally discovered by Cannon, Floyd, and Parry, gives us a new method for finding face pairing descriptions of 3-manifolds. In this paper, I will describe the construction in a way suitable for a more general audience than the original research papers, which include [2], [3], [4], and [5]. Along the way, I will describe Dehn Surgery and a set of moves which allows us to change the framings of a link without changing the topology of the manifold obtained by Dehn Surgery. Once the theory has been developed, I will apply it to find several bitwist representations of the Poincaré Sphere and 3-Torus. Finally, I discuss how one might attempt to find a set of moves that can take one bitwist representation of a manifold to any other bitwist representation of the same manifold.

Acknowledgments

First and foremost, I would like to thank Bill Floyd for all the time he spent helping me to understand the bitwist construction and more general concepts in low dimensional topology. I'd also like to thank Jim Thomson and Bud Brown for being on my committee, and being some of the best teachers I've had at Virginia Tech. I also thank Peter Linnell and Leslie Kay, for helping me out at various points during my time here.

Finally, I'd like to thank my family for supporting me always, especially in my studies of mathematics.

Contents

1	Introduction	1
2	Background Theory	2
	2.1 Manifolds	2
	2.2 Knots and Braids	3
	2.3 Dehn Surgery	6
	2.4 Twist Moves	10
	2.5 Cell Complexes and Face Pairings	14
3	The Bitwist Construction	16
4	Main Results of Bitwisted Face Pairings	20
	4.1 Corridor Complex Links	20
	4.2 Statement of Key Theorems	25
	4.3 Proof of the Construction	26
	4.4 Changing Edge Cycle Framings	28
	4.5 Proof of Main Result	30
5	Applications of Results to 3-Manifold Construction	31
	5.1 The Poincaré Sphere	31
	5.2 The 3-Torus	34
6	Equivalence of Bitwist Representations	37
	6.1 Equivalence of 3-Torus Representations	37
	6.2 Equivalence of Poincaré Sphere Representations	39
	6.3 Changing Multipliers	40
7	Further Research	41
	Bibliography	42

List of Figures

1	The trefoil knot	3
2	The trefoil as the closure of a braid (left), and as the closure of a pure braid (right)	3
3	The pure braid generator $B_{1,4}$	4
4	A full twist on four strands.	5
5	Two different types of crossing points	6
6	A torus with a parallel drawn in red and a meridian drawn in blue. The disk bounded by the meridian is shaded gray.	6
7	A: Taking a slice s of T_2 . B: Gluing s to a meridian m of T_1 , forming d_m . C: Two cylinders with tops and bottoms glued. We can collapsed them to two spheres with their boundaries glued, giving \mathbf{S}^3	7
8	A curve winding around a torus, before and after a single revolution twist.	10
9	How to change framings after a twist move. Here $s \in \mathbb{Z}$ and $r \in \mathbb{Q} \cup \{\infty\}$	11
10	Result of rotating three ribbons one clockwise revolution	12
11	A slam dunk. Here $n \in \mathbb{Z}$ and $q \in \mathbb{Q} \cup \{\infty\}$. It is important to keep in mind that this operation is reversible	13
12	Shaded grey is a strange looking 10-gon. Inside the 10-gon are two triangles.	15
13	A: A cube with faces opposite each other paired. B: The link of a vertex if the faces are paired by translation.	16
14	The model face pairing P	17
15	Q' , obtained by subdividing P , and Q , obtained by adding stickers to Q'	18
16	Edge components passing through a face component in f , through a tubular neighborhood of a path in the 1-skeleton, and into the interior of f'	21
17	The corridor complex link for the face pairing from Section 3	22
18	A partially drawn corridor complex link with a knotted edge component.	23
19	A link that looks like a corridor complex link, but is not.	24
20	Diagram representing the edge cycle $[e]$. Shaded bubbles represent which face we pass through. The multipliers of AB and BC are both $+1$	26
21	Diagram showing another edge cycle. The multipliers of AB , BC , and CD are -1 , 1 , and -1 respectively.	27
22	Adding alternating face and edge components to change the framing of an edge component from $2/7$ to 1	29

23	A: The trefoil knot represented by full twists with framing 1. B: A corridor complex link obtained from A. C: Changing the framing of an edge component so that the new framing is the reciprocal of an integer.	31
24	Applying Proposition 30 to the corridor complex link in Figure 23 C.	33
25	A faceted 3-ball described by Figure 24.	33
26	The Borromean Rings with framing 0	34
27	A: The Borromean Rings with framing 0 as the closure of a pure braids. B: The full twist representation of A	35
28	A: A corridor complex link obtained from Figure 27. B: A altered so that every framing is the inverse of an integer.	35
29	Applying Proposition 30 to the corridor complex link in Figure 28 B.	36
30	A faceted 3-ball obtained from Figure 29.	36
31	Using twist moves to go from the corridor complex link for the bitwist manifold constructed in Section 3 to the Borromean Rings with framing 0.	38
32	A: The corridor complex link for our third representation of the torus. B: Face pairing with the corridor complex link shown in A. Faces are paired by reflection.	39
33	A: Corridor complex link for a new representation of the Poincaré Sphere. B: Faceted 3-ball with face pairing for A. Faces are paired by reflection over their common edges.	40
34	A framed corridor complex link L	41

1 Introduction

In this paper, I will describe a new way of representing 3-manifolds called the bitwist construction. The construction was originally discovered by James Cannon, William Floyd, and Walter Parry through a fortunate mistake. It takes as input a faceted 3-ball plus a finite set of nonzero integers and produces a face pairing description of a closed, connected, orientable 3-manifold. Several years after the original construction was published, Cannon, Floyd, and Parry were able to modify the construction to its present form and prove that every closed, connected, orientable 3-manifold has a bitwist description.

Though it is well known that every closed, connected, orientable 3-manifold has a face pairing description, it is also known that in a sense face pairings which yield manifolds are rare (see [6]). Since the bitwist construction always yields a face pairing description of some 3-manifold, it helps to overcome this problem. The construction is also useful in that manifolds can be constructed and understood fairly quickly, especially with the use of computer software like SnapPea (see [12]). If nothing else, the bitwist construction is a fun tool for exploring 3-manifolds.

One sees that the bitwist construction can give every closed, connected, orientable 3-manifold by exploiting a relationship between the construction and Dehn Surgery. Much of this paper will be devoted to exploring that relationship. To do this, I first describe Dehn Surgery in Section 2.3. I go on in Section 2.4 to describe a set of procedures called twist moves which allows us to alter the framed surgery representation of a manifold. Using these moves on a special type of link, called a corridor complex link, we can find the bitwist representation of any 3-manifold that has a surgery representation. In Section 5 I show how to find bitwist representations of two important 3-manifolds, the Poincaré Sphere and the 3-Torus. Finally, in Section 6, I discuss how we might try to find a set of moves that can take one bitwist representation of a 3-manifold to any other bitwist representation of the same manifold. Unfortunately, on close examination it quickly becomes apparent that the answer to this question is likely to be quite complicated. As yet, whether such a set of moves exists is unknown.

In dimensions four or less, manifolds are usually studied by intuitive, geometric methods, rather than the more mechanical, algebraic methods which mathematicians have found to be very powerful in higher dimensions. Often proofs require the reader to be able to visualize the solution, as it is extremely difficult to describe in words a picture one sees in the mind's eye. I recommend that the reader of this, or any low dimensional topology paper, keep in mind that often the picture is better than the proof.

2 Background Theory

We begin by building up the basic theory necessary for understanding the bitwist construction. This section includes a discussion of manifolds, knots, Dehn Surgery, twist moves, and face pairings.

2.1 Manifolds

Definition 1. A manifold is a topological space M such that M is Hausdorff, 2^{nd} countable, and every point $p \in M$ has a neighborhood $U \subseteq M$ such that U is homeomorphic to an open subset of \mathbb{R}^n .

We are especially interested in *closed, connected, orientable 3-manifolds*. A manifold is *closed* if it is compact and *connected* if it is connected in the topological sense. Intuitively, we understand orientability as meaning that we can continuously designate a particular direction as “up.” If you were to live in a non-orientable 3-manifold, there would be some closed path you could follow so that when you return to your starting point your appearance has changed to be your mirror image. If you did this wearing only your right shoe while leaving your left shoe at the starting point, when you returned you would have two left shoes. A precise definition of orientability for 3-manifolds is below.

Definition 2. Let K be a solid cube, with the bottom of K glued to the top of K by a single reflection. We call K a Solid Klein Bottle. A 3-manifold M is non-orientable if it has a subspace homeomorphic to K . Otherwise, M is orientable.

We use the terminology *n-manifold* to indicate that each point in the manifold has a neighborhood homeomorphic to an open subset of \mathbb{R}^n . Finally, we say M is a *manifold with boundary* if M satisfies the axioms for a manifold except that each point has a neighborhood that is homeomorphic to an open subset of upper half-space, $\{(x_1, \dots, x_{n-1}, x_n) \in \mathbb{R}^n : x_n \geq 0\}$

Example 3. \mathbb{R}^n is trivially an n -manifold.

Example 4. The n -sphere $\mathbf{S}^n = \{(x_1, \dots, x_n, x_{n+1}) : x_1^2 + \dots + x_n^2 + x_{n+1}^2 = 1\}$ is an n -manifold, and is homeomorphic to $\widehat{\mathbb{R}}^n = \mathbb{R}^n \cup \{\infty\}$, the 1-point compactification of \mathbb{R}^n . We also have the n -ball, $\mathbf{B}^n = \{(x_1, \dots, x_n) : x_1^2 + \dots + x_n^2 \leq 1\}$, which is an n -manifold with boundary.

Note that most of the time, when we speak of something being “in \mathbf{S}^3 ” we realize \mathbf{S}^3 as $\widehat{\mathbb{R}}^3$.

Example 5. The n -torus $\mathbb{T}^n = \underbrace{\mathbf{S}^1 \times \mathbf{S}^1 \times \dots \times \mathbf{S}^1}_{n \text{ times}}$ is an n -manifold. We also often need the solid 2-torus, $\mathbf{S}^1 \times \mathbf{B}^2$, which is a 3-manifold with boundary.

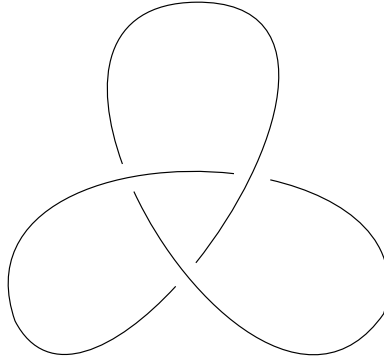


Figure 1: The trefoil knot

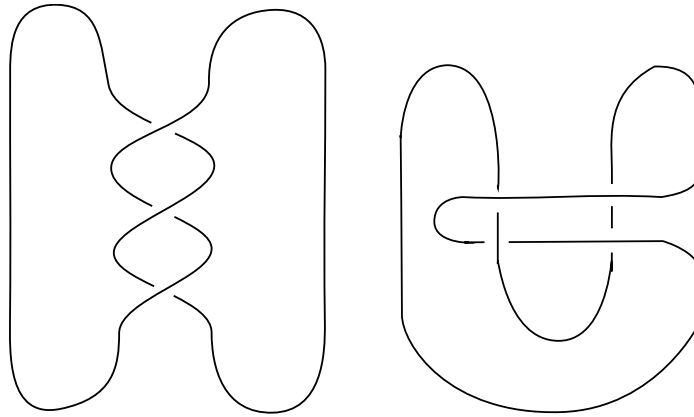


Figure 2: The trefoil as the closure of a braid (left), and as the closure of a pure braid (right)

2.2 Knots and Braids

Knots play an important role in the theory of 3-manifolds, and are essential to proving some of the most important theorems about bitwisted face pairings.

Definition 6. A knot is a smooth embedding of \mathbf{S}^1 into \mathbf{S}^3 . A link is a smooth embedding of the disjoint union of finitely many copies of \mathbf{S}^1 into \mathbf{S}^3 .

Knots do not in general need to be smooth, but by requiring them to be so we avoid the nasty problem of so-called “wild knots.”

A common example of a knot, called the trefoil, is in Figure 1. Although knots exist in \mathbf{S}^3 , we usually work with their planar projection into \mathbb{R}^2 or $\widehat{\mathbb{R}^2} \setminus \{\infty\}$, with certain parts of the curve cut out to indicate where the knot crosses under itself. We’ll call the knot which has no crossings in its planar projection the *unknot*. We say two knots are *equivalent* if there exists an orientation preserving isotopy of \mathbf{S}^3 taking the image of one knot to the image of the other.

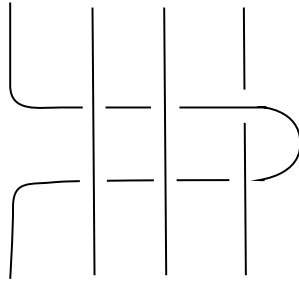


Figure 3: The pure braid generator $B_{1,4}$

Definition 7. A braid in n strands is a continuous one-parameter family of n points in \mathbb{R}^2 , say $f : [0, 1] \rightarrow (\mathbb{R}^2)^n$, such that for any $t \in [0, 1]$ no two points in the set of points defined by $f(t)$ are the same, $f(0) = \{(0, 1), (1, 1), \dots, (n-1, 1)\}$, and $f(1) = \{(y_1, 0), (y_2, 0), \dots, (y_n, 0) : y_1, \dots, y_n \in \{0, \dots, n-1\}, y_i \neq y_j \text{ if } i \neq j\}$.

We think of a braid as being a set of n curves in $\mathbb{R}^3 = \{(t, x, y)\}$, descending above from evenly spaced endpoints in $t = 0$ to an identical set of endpoints in $t = 1$. Sometimes we want to ensure that each curve descends from its endpoint in $t = 0$ to the endpoint directly below it in $t = 1$, which leads to the following.

Definition 8. A pure braid in n strands is a braid f in n strands with $f(1) = \{(0, 0), (1, 0), \dots, (n-1, 0)\}$.

As with links, we usually work with a braid's planar projection into \mathbb{R}^2 .

As one would expect, there is a way to turn a braid into a link.

Definition 9. A braid closure is a link formed from a braid by connecting pairs of endpoints by non-intersecting curves, which intersect the braid only at their endpoints.

See Figure 2 for both a braid and a pure braid representation of the trefoil knot. One can see that all three of these representations are equivalent by physically building the trefoil out of a shoe lace, and then manipulating it to get the braid and pure braid representations.

Braids and pure braids in n strands both have a group structure. In either case, elements of the group correspond to equivalence classes of braids (resp. pure braids), and there is a standard, finite presentation. For braids, the generating set for the braid group with n strands is the set $\{b_1, \dots, b_{n-1}\}$ where b_i corresponds to strand i and strand $i+1$ crossing each other, with strand i on top. For example, the trefoil in Figure 2 is a closure of the braid b_1^{-3} . The generators of the pure braid group with n strands are $\{B_{i,j} : i < j \leq n\}$ where $B_{i,j}$ represents strand i passing under any strands between i and j , over j , and then back under j and the other strands. See Figure 3 for an example. Further elaboration on braid groups can be found in chapter three of [10]. Perhaps the most important result found there is Alexander's Braiding Theorem, which says that every link is the closure

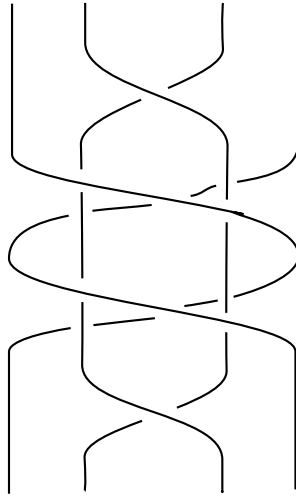


Figure 4: A full twist on four strands.

of some braid. With a bit of fiddling, we can turn any braid closure into a pure braid closure.

Proposition 10. *Every link is a closure of some pure braid.*

In the theory of bitwist manifolds, we are especially interested in pure braids that can be represented by full twists. A *full twist on n strands* is the pure braid you get by literally twisting n strands of rope by 2π in the counterclockwise direction. See Figure 4 for an example.

Proposition 11. *The pure braid group is generated by full twists.*

Proof. I will denote by $full_{i,j}$ a full twist on strands i through j , and by $full_{i,j}^{-1}$ its inverse. Also, define $full_{i,i}$ to be the identity. Now, $B_{i,j} = full_{i,j}$ trivially if $j = i + 1$, so assume $j > i + 1$. Thinking of $full_{i,j}$ as coming from physically twisting $j - i + 1$ strands by 2π , we see that $full_{i,j}^{-1}$ consists of an inverse full twist on strands $i + 1$ through j , along with strand i going first under the other strands and then over them. Hence, the pure braid described by $full_{i,j}^{-1}full_{i+1,j}$ consists of strand i going under all strands up to j , and then going back over them. Similarly, $full_{i,j-1}full_{i+1,j-1}^{-1}$ results in strand i going over all strands up to $j - 1$ and then going back under them. Putting it all together, we get $B_{i,j}^{-1} = full_{i,j}^{-1}full_{i+1,j}full_{i,j-1}full_{i+1,j-1}^{-1}$. Since $\{B_{i,j}\}$ generates the pure braid group, so does $\{full_{i,j}\}$. \square

As the proof above was constructive, Proposition 10 and Proposition 11 combine to give us a way of diagramming any link using full twists and inverse full twists.

Let J and K be two components of the same link. If K crosses over J in the link's planar projection, the crossing will be one of two different types, shown in Figure 5. Assigning the

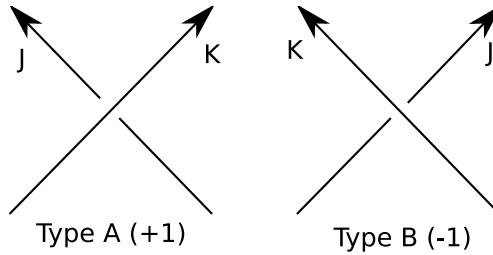


Figure 5: Two different types of crossing points

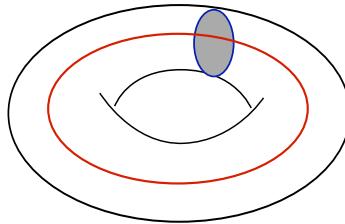


Figure 6: A torus with a parallel drawn in red and a meridian drawn in blue. The disk bounded by the meridian is shaded gray.

value $+1$ to type A and -1 to type B, we get one of the oldest knot invariants.

Definition 12. Let J and K be oriented components of the same link. Let $(\epsilon_1, \dots, \epsilon_n)$ be integers corresponding to the crossing points of J and K such that ϵ_i equals $+1$ if the crossing point is of type A and -1 if the crossing point is of type B. Then the Gauss linking number is $\text{lk}(J, K) = \sum \epsilon_i$.

2.3 Dehn Surgery

Dehn Surgery gives us a method of describing three manifolds using just links and rational numbers. The basic idea is to remove a solid torus from \mathbf{S}^3 , and then glue back a different solid torus by a homeomorphism of its boundary. We will see that every closed, connected, orientable 3-manifold can be obtained in this way. To introduce the idea, though, we have the following proposition.

Proposition 13. Let T be a solid torus standardly embedded in \mathbf{S}^3 . Then the closure of the complement of T is homeomorphic to another solid torus.

For the proof we need to define two special types of curves on the standardly embedded 2-Torus, called *meridians* and *parallels*. Informally, a parallel is a circle around the hole of the Torus and a meridian is a circle that goes through the hole. A *meridional disk* is a disk bounded by a meridian. A picture of a torus with a meridian and parallel drawn on it is shown in Figure 6.

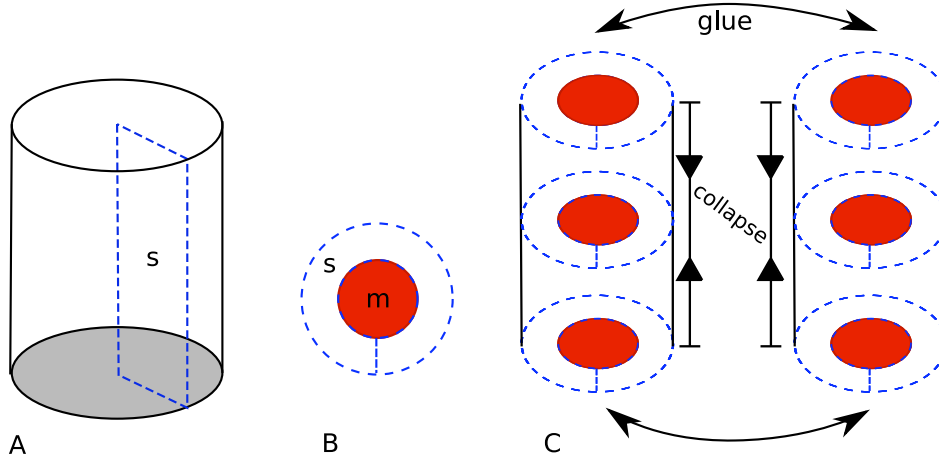


Figure 7: A: Taking a slice s of T_2 . B: Gluing s to a meridian m of T_1 , forming d_m . C: Two cylinders with tops and bottoms glued. We can collapsed them to two spheres with their boundaries glued, giving \mathbf{S}^3 .

Now we can prove Proposition 13.

Proof. Let T_2 be a solid torus standardly embedded in \mathbf{S}^3 , and T_1 another solid torus. Glue ∂T_1 to ∂T_2 by a homeomorphism that takes meridians to parallels and parallels to meridians. I will show that the resulting manifold is \mathbf{S}^3 . Throughout this proof, imagine T_1 as if it were standardly embedded in \mathbb{R}^3 .

Cut T_2 along a disk bounded by a meridian. The result is a cylinder with the top glued to the bottom, with parallels vertical line segments running from the top to the bottom. Choose some parallel l in T_2 , which is glued to a meridian m in T_1 . Considering T_2 as a cylinder, let s be the two dimensional slice of T_2 running through l to the line through the centers of the disks foliating T_2 . Then s is a rectangular strip with the top glued to the bottom, and one side glued to m . Thus, s can be attached to the disk bounded by m . This forms another disk, call it d_m .

Repeating this process, we get a disk d_m for every meridian m of T_1 . The boundary of any d_m is glued to the boundary of every other disk. Taken all together, we see that we have the quotient space of a torus, with each parallel in its own equivalence class. If we split the quotient space (thought of as a torus) into two cylinders with their tops and bottoms glued together, we see that we can collapse sides of the cylinders into a ring. This forms two 3-balls with their boundaries glued together, which is a well known representation of \mathbf{S}^3 .

So gluing T_1 to T_2 by a homeomorphism which takes meridians to parallels gives us \mathbf{S}^3 . But T_2 was standardly embedded in \mathbf{S}^3 , and the gluing leaves its geometry unchanged. Hence, T_1 must be homeomorphic to the closure of the complement of T_2 in \mathbf{S}^3 . \square

In fact, this proposition can be extended to say that the complement of any standardly

embedded handlebody of genus g in the 3-sphere is another handlebody of genus g . It is also true that for any closed, orientable 3-manifold, there exists $g \in \mathbb{N}$ such that for some embedding the complement of a handlebody with genus g is another handlebody with genus g . The division of a 3-manifold into two handlebodies is called a *Heegaard Splitting* (see [10] Chapter IV), and is the foundation on which much of the following theory is built.

What happens if we take the complement of a solid torus T in \mathbf{S}^3 , and then glue the torus back into $\mathbf{S}^3 - T$ by a different (non-isotopic) homeomorphism of its boundary? The result would still be a 3-manifold, but the topology would change. In fact, every closed, connected, orientable 3-manifold can be obtained by repeating this process a finite number of times, as stated by the following theorem.

Theorem 14. *Every closed, connected, orientable 3-manifold can be obtained by removing a finite number of solid tori from \mathbf{S}^3 and gluing them back in along different homeomorphisms of their boundaries. These tori can always be made to be unknotted.*

The above is given as a corollary to the Dehn-Lickorish Theorem in [10], which classifies homeomorphisms of surfaces. A full proof of the Dehn-Lickorish Theorem and its corollaries is well beyond our scope. However, we do need to classify the special case of curves on the boundary of a solid torus T . Choose a meridian α and parallel β on $\partial T = \mathbb{T}^2$. Let $\gamma = p\alpha + q\beta$ be a curve on ∂T that winds p times around α and q times around β . More precisely, γ represents an element of the fundamental group $\pi_1(\mathbb{T}^2) = \mathbb{Z} \times \mathbb{Z}$, and so can be considered as an equivalence class of curves.

Proposition 15. *Let $J = p\alpha + q\beta$ be a curve on \mathbb{T}^2 that is closed and non-intersecting. Then p and q are coprime, or one is 0 and the other is ± 1 .*

Proposition 16. *If two closed curves on the torus are homotopic, then they are isotopic.*

Taken together, these two propositions let us describe some homeomorphisms of the torus by rational numbers. We now turn to defining exactly what is meant by the meridian and parallel on an embedded torus. We've already done this on a standardly embedded torus (Figure 6), but we'd like to generalize to other embeddings.

The meridian is easily generalized, and in fact looks exactly the same in any embedding of the torus. To understand how we define the parallel in general, imagine the standardly embedded torus as a non-overlapping piece of rope lying flat on a table. Choose a meridian and a parallel. Now imagine twisting the torus by a half twist, so that the torus crosses over itself once. This causes the parallel to wind once around the meridian of the torus. If we do a full twist, the parallel will wind around twice. Now imagine sliding the right side of the torus over the left side. In this case, the parallel does not wind around the meridian at all.

In each of the cases above, there is at least one invariant. The linking number of the parallel J and a curve running through the center of the torus K is 0. This fact gives rise to the

definition of a parallel that works for any embedding of the torus.

Definition 17. *Let T be a tubular neighborhood of a knot in \mathbf{S}^3 . Let J be a closed curve on T , and let K be the closed curve traveling through the centers of meridional disks of T . Then J is a parallel for T if:*

1. J and K are codirected (any two vectors on the curves pointed in the direction of orientation have positive inner product).
2. $\text{lk}(J, K) = 0$

We're now ready to describe *Dehn Surgery*. Let L be a link in \mathbf{S}^3 , and let J be a link component. We assign to J a number $r = p/q \in \mathbb{Q} \cup \{\infty\}$ called a *framing*. Thicken J to a solid torus, which we will also call J , and let γ be a curve on ∂J so that $\gamma = p\alpha + q\beta$. Let T be another solid torus, and m a meridian of T . By Dehn Surgery, we mean the operation of gluing T to $\mathbf{S}^3 \setminus J$ by a boundary homeomorphism taking m to γ . Note that by the corollary to the Dehn-Lickorish Theorem 14, every closed, connected, orientable 3-manifold is obtained by performing Dehn Surgery on every component of some link L .

To see that this homeomorphism exists, let $\gamma' = \alpha$ be a curve around the meridian. Say we want a homeomorphism h of \mathbb{T}^2 that takes γ' to $\gamma = p\alpha + q\beta$, where $p, q \in \mathbb{Z}$ are coprime or one is 0 and the other is ± 1 . Then $\exists a, b \in \mathbb{Z}$ such that $ap - bq = 1$, and the matrix $A = \begin{pmatrix} p & b \\ q & a \end{pmatrix}$ is in $\text{SL}(2, \mathbb{Z})$. The torus is homeomorphic to \mathbb{R}^2/\mathbb{Z} and the inverse of A has integer entries, so A induces a homeomorphism of \mathbb{T}^2 . Representing γ' and γ as matrices, we see that

$$A \begin{pmatrix} 1 \\ 0 \end{pmatrix} = \begin{pmatrix} p & b \\ q & a \end{pmatrix} \begin{pmatrix} 1 \\ 0 \end{pmatrix} = \begin{pmatrix} p \\ q \end{pmatrix}$$

and so h is the homeomorphism induced by A . Note that due to Propositions 15 and 16, our exact choice of curves γ' and γ does not matter as long as they each wind around the meridian and parallel the correct number of times.

Given the planar projection of an unframed link, there is a standard way to frame it, called the *blackboard framing*. Convert a given link component J into a ribbon lying flat against the "blackboard." We think of one edge of the ribbon as being the original link component J , and the other edge as being a new link component K . The blackboard framing for J is equal to $\text{lk}(J, K)$. Note that the blackboard framing may not be the same for equivalent links.

It is in fact possible to represent any integer framing as a ribbon. If we consider the planar projection of link component J as one edge of the ribbon and K as the other edge, then K represents a curve γ on the boundary of the solid torus obtained by thickening J . The ribbon then represents the framing $p = \text{lk}(J, K)$. For example, if the ribbon does not lie

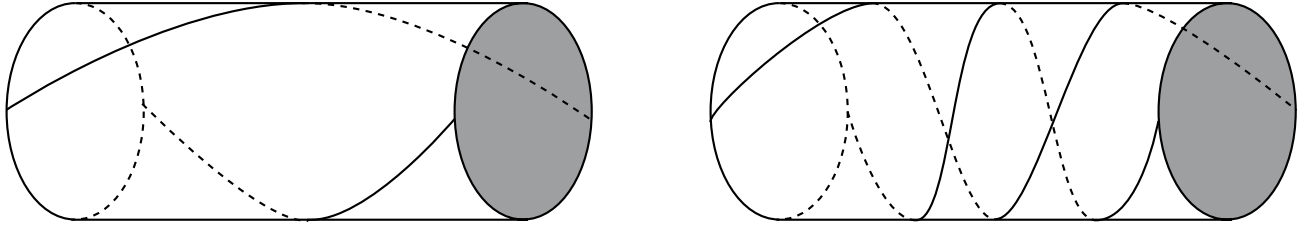


Figure 8: A curve winding around a torus, before and after a single revolution twist.

flat in the plane but rather twists so that $\text{lk}(J, K) = 0$, then K is the parallel for J and the ribbon represents a link component with framing 0. By adding extra twists to the ribbon, we can represent Dehn Surgery by any integer framing.

2.4 Twist Moves

Our goal in this section is to describe a set of operations which I will refer to as twist moves or Rolfsen Twists. We want to be able to manipulate framed links, both in terms of changing the framing and changing the link itself, in such a way that the manifold obtained by Dehn Surgery remains the same. Collectively, these moves create the Kirby Calculus, which can take any framed surgery representation of a manifold to any other framed surgery representation of the same manifold.

First, we need to define a special type of homeomorphism of the solid torus.

Definition 18. *Cut a solid torus T along a meridional disk, so that the torus becomes a cylinder with the top glued to the bottom. Rotate one end of the cylinder by 2π , and then glue it back to the other end of the cylinder. Since after twisting points at the two ends of the cylinder match back up, this describes a homeomorphism called a twist along a meridional disk or Dehn Twist. If we rotate instead by $2n\pi$, $n \in \mathbb{Z}$, then the homeomorphism is a twist of n revolutions. The sign of n determines whether we twist in the direction of or opposite the direction of a chosen orientation.*

For the remainder of this section, we choose our orientations so that twisting in the positive direction is a clockwise twist.

Now we will prove several methods of altering the framings of a link. Collectively, we call the following propositions *twist moves*.

Proposition 19. *Let J be the unknot embedded in \mathbf{S}^3 , let $r \in \mathbb{Q} \cup \{\infty\}$, and let $n \in \mathbb{Z}$. Then the manifold obtained by Dehn Surgery on J with framing r is homeomorphic to the manifold obtained by Dehn Surgery on J with framing $r' = \frac{1}{n + \frac{1}{r}}$.*

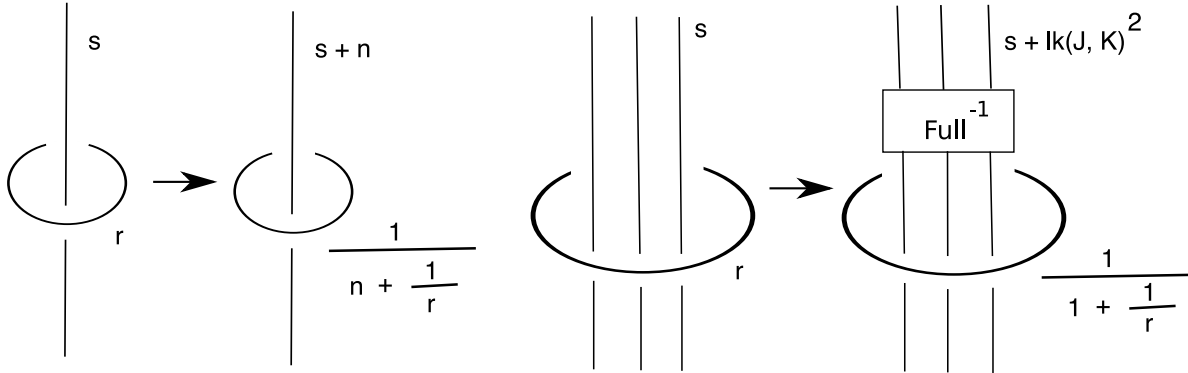


Figure 9: How to change framings after a twist move. Here $s \in \mathbb{Z}$ and $r \in \mathbb{Q} \cup \{\infty\}$

Proof. Thicken J so that it becomes a solid torus, which we will also denote by J . Then the closure of the complement of J in \mathbf{S}^3 is another solid torus, T_2 . Write $r = p/q$, where p and q are coprime. Fix a meridian and parallel on T_2 , which we will denote by α and β respectively. Since parallels are glued to meridians, r describes the curve $q\alpha + p\beta$ on ∂T_2 . Hence, we can describe the surgery operation as gluing the meridian of a torus T_1 to the curve $\gamma = q\alpha + p\beta$ on T_2 .

Pick a meridian of T_2 , and notice that γ intersects the meridian at exactly p points. Now perform a twist of n revolutions on $T_2 = \mathbf{S}^3 \setminus J$. After twisting, γ winds around the meridian exactly $q + np$ times (see Figure 8). The number of times γ winds around the longitude remains unchanged, so after twisting we've obtained $\gamma' = (q + np)\alpha + p\beta$.

Now, let M be the manifold obtained by gluing a T_1 to T_2 along γ . Then since twisting is a homeomorphism of T_2 , gluing T_1 along γ' yields a manifold homeomorphic to M .

By its definition, γ' describes a curve on J , namely the curve $p\alpha + (q + np)\beta$. This describes a framing:

$$r' = \frac{p}{q + np} = \frac{1}{\frac{q}{p} + n} = \frac{1}{\frac{1}{r} + n}$$

□

We now consider an unknot in \mathbf{S}^3 with a single strand from another knot passing through it. The following theorem is shown pictorially in Figure 9.

Proposition 20. *Let J be the unknot and K be another knot such that a single strand of K passes through J . If J has framing $r \in \mathbb{Q} \cup \{\infty\}$ and K has framing $s \in \mathbb{Z}$, then changing the framing of J to $r' = \frac{1}{\frac{1}{r} + n}$ and the framing of K to $s' = s + n$ does not change the topology of the manifold obtained by Dehn Surgery.*

Proof. Let D be a closed disk with boundary J . Thicken J and K to solid tori while shrinking

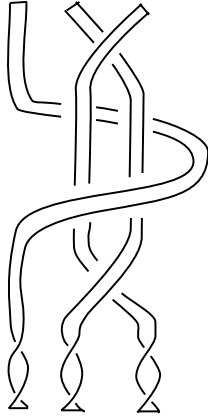


Figure 10: Result of rotating three ribbons one clockwise revolution

D , so that the boundary of D is a meridional disk of K and ∂D is a parallel of J . Then rotating D by $2n\pi$ induces a homeomorphism of $\overline{\mathbf{S}^3 \setminus J}$, since D is also a meridional disk of $\overline{\mathbf{S}^3 \setminus J}$. We examine the effect of twisting to understand how we can change our framings.

Now, s is an integer, so the curve $\gamma_J = s\alpha + 1\beta$ intersects D exactly once. Hence, rotating D by $2n\pi$ changes the framing of K to $s' = s + n$.

Since rotating D was a Dehn Twist on $\overline{\mathbf{S}^3 \setminus J}$, by the argument used in Proposition 19 the framing of J changes to $r' = \frac{1}{\frac{1}{r} + n}$.

□

With a bit of work, the ideas from above can be adapted to show what happens when several strands from the same link component pass through an unknot. Again, see Figure 9 for the picture.

Proposition 21. *Let J be the unknot and K be a different link component. If J has framing $r \in \mathbb{Q} \cup \{\infty\}$ and K has framing $s \in \mathbb{Z}$, then changing the framing of J to $r' = \frac{1}{\frac{1}{r} + n}$, the framing of K to $s' = s + \text{nlk}(J, K)^2$, and adding n inverse full twists (or n full twists if $n < 0$) to the strands of K passing through J does not change the topology of the manifold obtained by Dehn Surgery.*

Proof. We represent integer surgery on K by a ribbon in \mathbb{R}^2 , as described at the end of Section 2.3. We orient \mathbb{R}^2 clockwise, which induces an orientation on K . We say K has a strands passing through J in one direction, and b strands in the opposite direction (Here we take “direction” to mean up or down). As in the proof of Proposition 20, we rotate the closed disk with boundary J by $2n\pi$ which changes the framing of J to $r' = \frac{1}{\frac{1}{r} + n}$. For

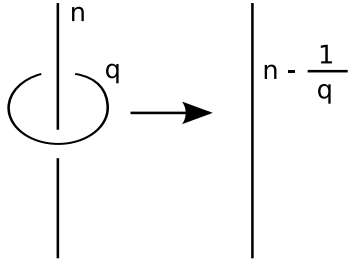


Figure 11: A slam dunk. Here $n \in \mathbb{Z}$ and $q \in \mathbb{Q} \cup \{\infty\}$. It is important to keep in mind that this operation is reversible

now, let $n = 1$, so that the ribbons representing K are given a single inverse full twist, and in addition each ribbon is twisted clockwise around itself once (Figure 10).

We first consider how the inverse full twist on the ribbons of K changes the framing. In an inverse full twist on $a+b$ strands, each ribbon passes over $(a+b)-1$ other ribbons. Checking the definition of $\text{lk}(J, K)$ (Definition 12) and a full twist (Figure 4) we see that each time a ribbon passes over another going in the same direction the framing of K changes by $+1$, and each time a ribbon passes over another going in the opposite direction the framing of K changes by -1 . So each strand in the s direction contributes $a-1-b$ to the new framing, and taken together they contribute $a(a-1-b) = a(a-1) - ab$. Likewise, the strands in the t direction contribute $b(b-1-a) = b(b-1) - ba$.

Each ribbon is also twisted around itself once in the clockwise direction. This contributes $+1$ to the new framing for each ribbon, regardless of direction. In total we get a contribution of $a+b$. Putting all of these contributions together, we see that our new framing is

$$s' = s + a(a-1) - ab + b(b-1) - ba + a + b = s + a^2 + b^2 - 2ab = s + (a-b)^2$$

But $(a-b) = \text{lk}(J, K)$, so we see that the new framing is $s' = s + \text{lk}(J, K)^2$.

Now, if we let n be any positive integer, we get n inverse full twists and each ribbon is twisted around itself n times clockwise. Hence, the new framing is $s + n\text{lk}(J, K)^2$. If n is negative, we get n full twists and each ribbon is twisted around itself n times counterclockwise. Repeating the above calculations, we see that the new framing is still $s + n\text{lk}(J, K)^2$. \square

Note that Proposition 21 can be generalized to the case where strands from several different link components pass through J . In that case, we add a full twist and change the framing of J as normal, but we calculate the new framings of each different link component separately.

There is one more move we need, called a *slam dunk*. It gives us new options for handling link components with rational framing. The move is described pictorially in Figure 11.

Proposition 22. *Let J be an unknot and K a different link component such that a single strand of K passes through J . If the framing of J is $r \in \mathbb{Q} \cup \{\infty\}$ and the framing of K is $s \in \mathbb{Z}$, then removing J and changing the framing of K to $s' = s - \frac{1}{r}$ does not change the topology of the manifold obtained by Dehn Surgery.*

See [7] page 163 for more information about slam dunks.

2.5 Cell Complexes and Face Pairings

In this section I will define cell complexes and face pairings. Much of it will be informal, as in most cases we can let our intuition guide us. More rigorous discussions of cell complexes and face pairings can be found in [11] and [8]. For the bitwist construction, we are interested in cell complexes that are somewhere in between CW-complexes and regular complexes in terms of generality.

Definition 23. *An n -cell is a topological space homeomorphic to \mathbf{B}^n . In this context, we define \mathbf{B}^0 to be a single point.*

We call a 0-cell a *vertex*, a 1-cell an *edge*, and a 2-cell a *face*. A *cell complex on \mathbf{B}^3 or faceted 3-ball P* is a cell structure such that:

1. There is one and only one 3-cell. Thus P is homeomorphic to \mathbf{B}^3 .
2. The boundary of an n -cell is the union of $(n - 1)$ -cells.
3. The union of n -cells where $n \leq 1$ is connected. This is the same as saying that the *1-skeleton* of P is connected.

We place additional restrictions on what faces are allowed. For f to be a face of P , there must exist a convex n -gon c consisting of one face, n edges, and n vertices such that:

1. There is a continuous, surjective map $h : c \rightarrow f$.
2. For each open n -cell d in c , the restriction of h is a homeomorphism of d to an n -cell in f .

If c is an n -gon, then we refer to f as an n -gon as well. Note that this means we may be counting some edges of f twice. A good example of a strange-looking face allowed by our definition is in Figure 12.

Assume from this point on that faceted 3-balls always have 0 or an even number of n -gons for all n , so that we can group the n -gons in pairs. A *face pairing* ϵ on a faceted 3-ball P is a collection of continuous maps of faces, $(\epsilon_1, \epsilon_2, \dots, \epsilon_m)$, one for each pair of faces in P . In addition, we must take care when constructing each ϵ_i .

Say an n -gon f is paired with f' . Form a cell complex g by barycentrically subdividing f .

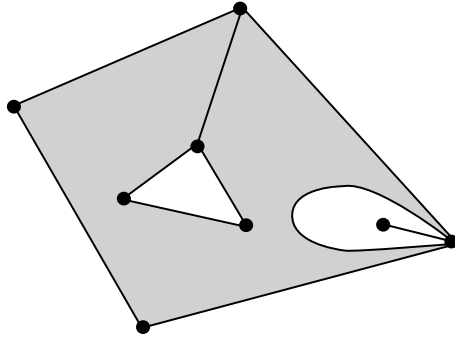


Figure 12: Shaded grey is a strange looking 10-gon. Inside the 10-gon are two triangles.

Then g is the union of triangles. Form g' from f' in a similar fashion. Then ϵ_i must restrict on a triangle of g to an orientation reversing homeomorphism to a triangle in g' . In addition, ϵ_i must take edges to edges and vertices to vertices in a way which satisfies the face pairing compatibility condition

$\epsilon = (\epsilon_1, \epsilon_2, \dots, \epsilon_m)$ canonically describes an equivalence relation on P , where $x \sim y$ if $\epsilon_i(x) = y$ for some i . For the sake of brevity, we will sometimes refer to a faceted 3-ball P with face pairing ϵ as $P(\epsilon)$.

The topology of P/ϵ is entirely determined by the permutation of the edges of P induced by each component ϵ_i of ϵ . For this reason, we will generally describe ϵ_i in permutation notation with letters representing vertices. If necessary, we will include numbers to eliminate ambiguity. For example, writing

$$\epsilon_1 : \begin{pmatrix} A & B & 1 & C \\ D & A & 6 & E \end{pmatrix}$$

means that ϵ_1 takes edge AB to edge DA , edge $B1C$ to edge $A6E$, and edge CA to edge ED .

The quotient space formed by a face pairing on a faceted three ball will not always be a manifold. In fact, there is evidence to suggest that in the space of all possible face pairings, the subset of face pairings that yield manifolds has measure 0 (see [6]). To tell whether the quotient space of a face pairing is a manifold, we can check the *vertex links* of the quotient space. A vertex link is the boundary of a sufficiently small neighborhood of a vertex. The following classical result can be found on page 121 of [11], and says that the only place the quotient space of a face pairing can fail to be a manifold is at the vertices.

Theorem 24. *Let P be a faceted 3-ball with face pairing ϵ . Then $M = P(\epsilon)$ is a manifold if and only if every vertex link of M is \mathbf{S}^2 .*

Now, consider the face pairing on the faceted 3-ball P shown in Figure 13 A. If we assume

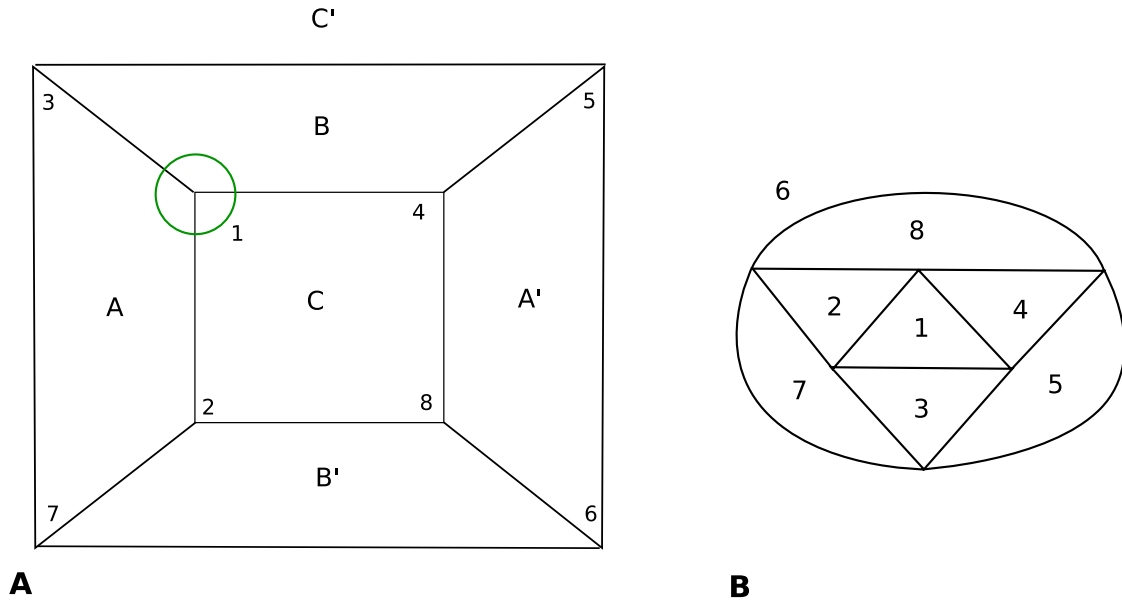


Figure 13: A: A cube with faces opposite each other paired. B: The link of a vertex if the faces are paired by translation.

the faces to be paired by translation, we get the 3-torus. In the quotient space there is only one vertex, and in Figure 13 B we calculate its link to be S^2 by looking at how triangles enclosing the eight vertices of P glue together in the quotient space.

If instead we take face A to be paired with A' by translation followed by a $1/4$ twist, B to be paired with B' likewise, and C to be paired with C' by translation, then the quotient space is not a manifold. We once again have only one vertex, but by examining triangles enclosing the eight vertices in P we will quickly find that they do not glue together to form a 2-sphere in the quotient space.

If a face pairing does form a manifold M , then M will always be a closed, connected, orientable 3-manifold. M is closed and connected because it is the quotient of \mathbf{B}^3 , which is compact and connected. M is orientable because we required the components of the face pairing ϵ to be orientation reversing.

3 The Bitwist Construction

In this section, we describe the bitwist construction. As mentioned in Section 2.5, a face pairing of \mathbf{B}^3 does not usually yield a 3-manifold. The bitwist construction gives us a way of creating face pairing descriptions of closed, orientable 3-manifolds, given just a base face pairing and a set of nonzero integers. I will describe the construction through an example.

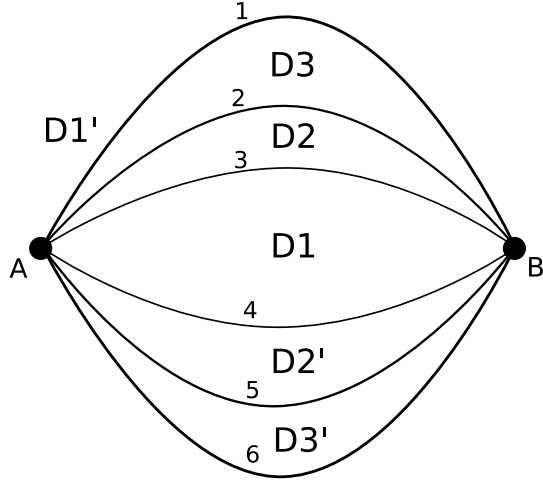


Figure 14: The model face pairing P

We begin with a faceted 3-ball P with face pairing ϵ . P consists of six digons and is shown in Figure 14. ϵ pairs face $D1$ with $D1'$, $D2$ with $D2'$, and $D3$ with $D3'$. Each pair of faces corresponds to maps ϵ_1 , ϵ_2 , and ϵ_3 respectively. In permutation notation, the maps are given by:

$$\epsilon_1 : \begin{pmatrix} A & 3 & B & 4 \\ A & 1 & B & 6 \end{pmatrix} \quad \epsilon_2 : \begin{pmatrix} A & 2 & B & 3 \\ A & 5 & B & 4 \end{pmatrix} \quad \epsilon_3 : \begin{pmatrix} A & 1 & B & 2 \\ A & 6 & B & 5 \end{pmatrix}$$

Collectively, these maps define a face pairing ϵ , giving rise to edge cycles:

$$\begin{aligned} A3B &\xrightarrow{\epsilon_1} A1B \xrightarrow{\epsilon_3} A6B \xrightarrow{\epsilon_1^{-1}} A4B \xrightarrow{\epsilon_2^{-1}} A3B \\ A2B &\xrightarrow{\epsilon_2} A5B \xrightarrow{\epsilon_3^{-1}} A2B \end{aligned}$$

The first edge cycle has length $\ell([A3B]) = 4$ and the second edge cycle has length $\ell([A2B]) = 2$. The bitwist construction requires that for each edge cycle we choose a *multiplier*, which is an arbitrary, nonzero integer. Here we choose $\text{mul}([A3B]) = -1$ and $\text{mul}([A2B]) = 1$. Now we subdivide each edge in an edge cycle $[e]$ into $|\text{mul}([e])| \cdot \ell([e])$ edges by adding vertices, creating a new faceted 3-ball Q' . See Figure 15 for Q' in our example.

Considering \mathbf{S}^2 as the boundary of \mathbf{B}^3 , we see that a choice of orientation on \mathbf{B}^3 induces an orientation on P . We can choose either orientation of \mathbf{B}^3 for the bitwist construction. For this example, we choose to orient \mathbf{B}^3 so that each face in P is oriented in the clockwise direction. Each face then induces an orientation on the edges in the boundary of the face.

We can now obtain a faceted 3-ball Q from Q' as follows. For an edge e , we say that it has *target* vertex v if v is the endpoint of e that we would reach if we traveled along e from

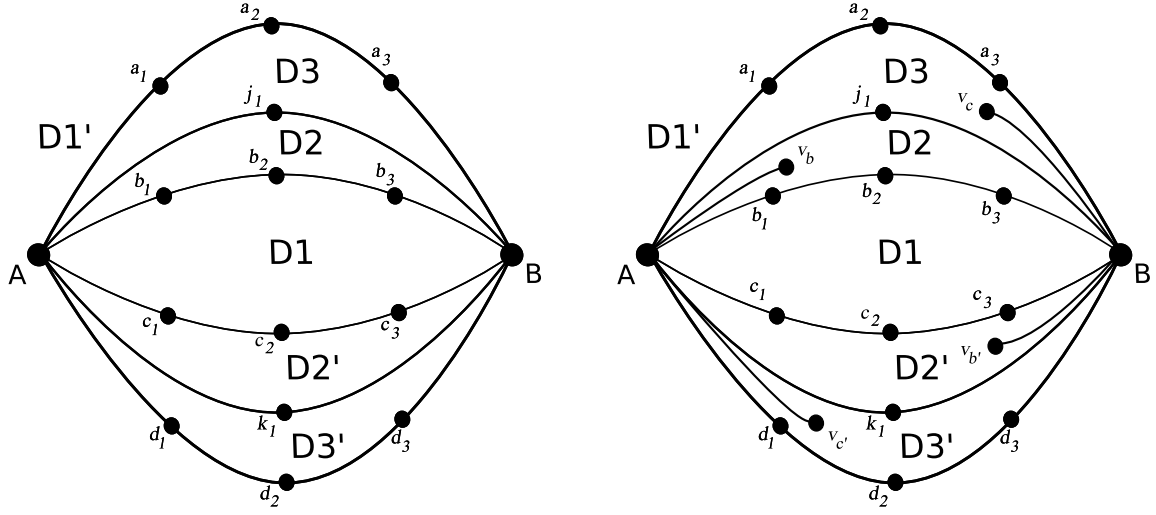


Figure 15: Q' , obtained by subdividing P , and Q , obtained by adding stickers to Q'

its center in the direction of its orientation. We say the other endpoint of e is the *source* vertex of e . Let f be a face of Q , let v be a vertex of f , and let e_1, e_2 be adjacent edges of f . If e_1 has target v with $\text{mul}([e_1]) < 0$ and if e_2 has source v with $\text{mul}([e_2]) > 0$, then we add a *sticker* to f at v . A sticker is an additional edge with one endpoint at v and the other endpoint in the interior of f . In our example, since we have $\text{mul}([A3B]) < 0$ and $\text{mul}([A2B]) > 0$ we add four stickers to obtain Q , as shown in Figure 15. In the future, we will refer to edges of P as *original edges* and edges of Q as *new edges* or just *edges*. Although stickers do not appear as part of the subdivision of any original edge, we will treat them as part of the subdivision of both original edges they are connected to.

The bitwist construction obtains a manifold from Q by “twisting” ϵ . Informally, a *positive twist* on an original edge e sends each edge in the subdivision of e in Q to the edge which follows it going opposite the direction of orientation. Similarly, a *negative twist* on e sends each edge in the direction of orientation. We obtain a face pairing δ from ϵ by post-composing ϵ with a positive twist if $\text{mul}([e]) > 0$, or a negative twist if $\text{mul}([e]) < 0$. For a more precise and rigorous description of how δ is obtained, see [5]. In our example, the edge permutations δ_1, δ_2 , and δ_3 , obtained from twisting ϵ on Q , are defined as follows:

$$\delta_1 : \begin{pmatrix} A & b_1 & b_2 & b_3 & B & c_3 & c_2 & c_1 \\ d_1 & A & a_1 & a_2 & a_3 & B & d_3 & d_2 \end{pmatrix} \quad \delta_2 : \begin{pmatrix} b_1 & A & v_b & A & j_1 & B & b_3 & b_2 \\ c_2 & c_1 & A & k_1 & B & v_{b'} & B & c_3 \end{pmatrix}$$

$$\delta_3 : \begin{pmatrix} j_1 & A & a_1 & a_2 & a_3 & B & v_c & B \\ A & v_{c'} & A & d_1 & d_2 & d_3 & B & k_1 \end{pmatrix}$$

Notice that the purpose of the stickers is to make δ well defined. We’ve placed stickers so that for every sticker there is a positive and a negative edge mapped to it by δ . This resolves

a conflict caused by allowing twists in two different directions. Without adding the stickers, all of the multipliers would have to have the same sign.

δ gives rise to edge cycles:

$$\begin{aligned}
b_1 b_2 &\xrightarrow{\delta_1} A a_1 \xrightarrow{\delta_3} v_c A \xrightarrow{\delta_C^{-1}} A j_1 \xrightarrow{\delta_2} k_1 B \xrightarrow{\delta_3^{-1}} B v_c \xrightarrow{\delta_3} d_3 B \xrightarrow{\delta_1^{-1}} c_2 c_3 \xrightarrow{\delta_2^{-1}} b_1 b_2 \\
a_2 a_3 &\xrightarrow{\delta_3} d_1 d_2 \xrightarrow{\delta_1^{-1}} A c_1 \xrightarrow{\delta_2^{-1}} v_b A \xrightarrow{\delta_2} A k_1 \xrightarrow{\delta_3^{-1}} j_1 B \xrightarrow{\delta_2} B v_b \xrightarrow{\delta_2^{-1}} b_3 B \xrightarrow{\delta_1} a_2 a_3 \\
A b_1 &\xrightarrow{\delta_1} d_1 A \xrightarrow{\delta_3^{-1}} a_2 a_1 \xrightarrow{\delta_1^{-1}} b_3 b_2 \xrightarrow{\delta_2} B c_3 \xrightarrow{\delta_1} a_3 B \xrightarrow{\delta_3} d_2 d_3 \xrightarrow{\delta_1^{-1}} c_1 c_2 \xrightarrow{\delta_2^{-1}} A b_1
\end{aligned}$$

To see that M is a manifold, we could check vertex links. An easier method, though, is to use the Euler Characteristic.

Definition 25. *Let P be a faceted 3-ball with face pairing ϵ . Let c_0 be the number of vertices of P / ϵ , c_1 the number of edges, c_2 the number of faces, and c_3 the number of 3-cells. Then the Euler Characteristic χ for P / ϵ is $\chi(P / \epsilon) = c_0 - c_1 + c_2 - c_3$.*

With some algebraic topology, it can be proved that the Euler Characteristic is well defined, in that homeomorphic quotient spaces will have the same Euler Characteristic. The above definition defines the Euler Characteristic for face pairing quotients in three dimensions, but it is worth noting that it can be generalized to face pairings in an arbitrary finite dimension. In fact, in two dimensions all that is needed to classify a closed, connected manifold up to homeomorphism is knowing whether it is orientable and its Euler Characteristic. For us, the Euler Characteristic is useful because of the following classical result, a proof of which can be found in [11].

Theorem 26. *Let P be a faceted 3-ball with face pairing ϵ . Then P / ϵ is a manifold if and only if $\chi(P / \epsilon) = 0$.*

Define $M = Q / \delta$. Then M clearly has a single 3-cell and three faces. Each edge cycle of δ represents a single edge in Q / δ so we get three edges. By inspecting the edge cycles we see that every vertex is equivalent to every other vertex, so we have a single vertex. Hence the Euler Characteristic $\chi(M) = 1 - 3 + 3 - 1 = 0$, and M is a manifold. In fact, we will prove later that any quotient space obtained by the bitwist construction is a manifold by showing that the Euler Characteristic is always zero.

We can find the fundamental group of M using a classical theorem about face pairings.

Theorem 27. *Let Q be a faceted three ball with face pairing δ . Then the fundamental group of $M = \mathbf{B}^3 / \delta$ has generators x_1, x_2, \dots , one for each face of M , and relators W_1, W_2, \dots given by edge cycles as described below.*

We see that in our example we have three generators, call them x_1, x_2 , and x_3 . To get relators, we simply pull off the maps above the arrows in the edge cycles, replacing δ with

x. We get:

$$\begin{aligned} W_1 &= x_1 x_3 x_3^{-1} x_2 x_3^{-1} x_3 x_1^{-1} x_2^{-1} = [x_1, x_2] \\ W_2 &= x_3 x_1^{-1} x_2^{-1} x_2 x_3^{-1} x_2 x_3^{-1} x_1 = [x_3, x_1^{-1}] \\ W_3 &= x_1 x_3^{-1} x_1^{-1} x_2 x_1 x_3 x_1^{-1} x_2^{-1} = [x_3^{-1}, x_2] \quad (\text{using } W_2) \end{aligned}$$

So we see that M has fundamental group $\mathbb{Z} \times \mathbb{Z} \times \mathbb{Z} = \pi_1(\mathbb{T}^3)$. Later we will prove that M is in fact the 3-torus.

4 Main Results of Bitwisted Face Pairings

4.1 Corridor Complex Links

Before I discuss the most important results to date, we need to define a special type of link called a *corridor complex link* which is determined by a face pairing on a faceted 3-ball. Let $P(\epsilon)$ be a faceted 3-ball with a face pairing ϵ . I will define L , a corridor complex link for P , by describing its planar projection into $\partial P = \mathbf{S}^2$. My description will differ from the description originally given in [4], in that I do not construct a corridor complex before constructing a corridor complex link. Assume throughout this discussion that the point at infinity in P has been placed so that the planar projection of L lies in $\mathbf{S}^2 \setminus \{\infty\}$.

Let f and f' be two faces of P paired by ϵ . Then L has an unknot component on the interior of f , called a *face component*. For each edge e of f , there is a single strand in L running from the barycenter of e through the face component. These strands must be drawn such that they do not overlap within the interior of f , and they all must pass through the unknot in the same direction. We call the strands *edge component strands*.

Now, pick a vertex v of f , and let v' be the vertex of f' paired with v by ϵ . Since the 1-skeleton of P is connected, there exists a path in the 1-skeleton from v to v' . The edge component strands, after going through the unknot in f , pass through a small tubular neighborhood of this path from v to v' and into the interior of f' . Then each edge component strand travels to the barycenter of a different edge of f' . Throughout this whole process, we still require that the edge component strands do not intersect. See Figure 16 to see a general example of the construction above.

If we add face components and edge component strands for every face pair in P , we get a link. Edge component strands never cross on the interior of a face, nor do they ever cross while passing through the tubular neighborhood of the 1-skeleton. The only time they may cross is when an edge component strand on the interior must cross edge component strands passing through a tubular neighborhood of the 1-skeleton, in which case the edge component strands in the tubular neighborhood cross over the strand in the interior. Eventually the

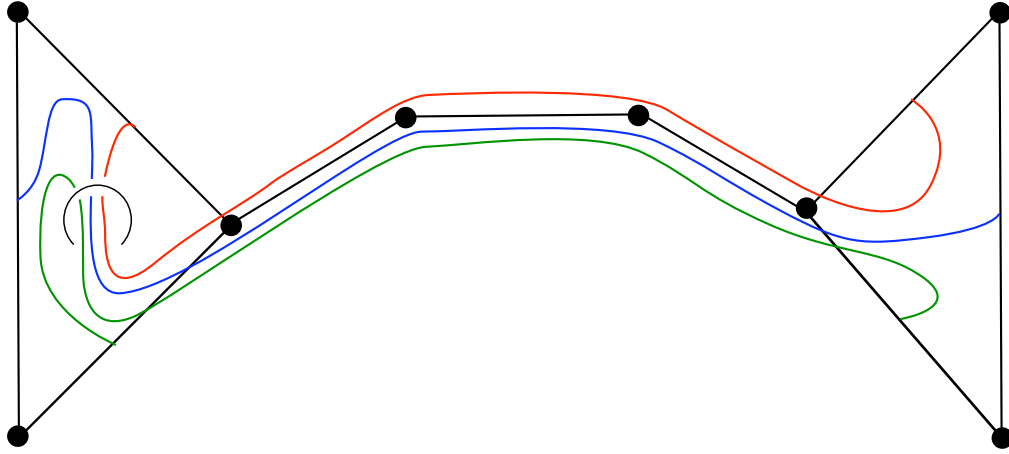


Figure 16: Edge components passing through a face component in f , through a tubular neighborhood of a path in the 1-skeleton, and into the interior of f'

edge component strands close to become link components of L , called *edge components*. In fact, L has exactly one edge component for each edge cycle of $P(\epsilon)$.

If a face component has two edge components passing through it, we call that face component a *digon face component*. We similarly define *triangle face components*, *quadrilateral face components*, etc.

The corridor complex link for the face pairing $P(\epsilon)$ from Section 3 is shown in Figure 17. Notice that the edge components correspond with the edge cycles, in that there is one edge component per edge cycle. Also, edge components pass through face components corresponding to faces in the edge cycle.

Corridor complex links can become quite complicated, and even have knotted edge components. An example of a corridor complex link with a knotted edge component is shown in Figure 18.

How can we tell when a link is a corridor complex link? This is a deceptively difficult question to answer. For example, shown in Figure 19 is a link which looks like it should be the corridor complex link for some faceted 3-ball. In fact, it is not a corridor complex link for any face pairing.

Consider the link L in Figure 19. Say $P(\epsilon)$ is a faceted 3-ball with face pairing ϵ that has corridor complex link L . We will show that $P(\epsilon)$ does not exist. Since L has two face components and two edge components, we know P has four digons. Pick a pair of digons, which are mapped to each other by ϵ . Any pair of digons either shares two edges, a single edge or no edges. If they share two edges, then one digon is the complement of the interior of the other, and we have nowhere left to fit the other pair of digons. If they share no edges, then one can calculate that only one faceted 3-ball P is possible and under any face pairing the corridor complex link for $P(\epsilon)$ is not L . If they share exactly one edge, then the corridor

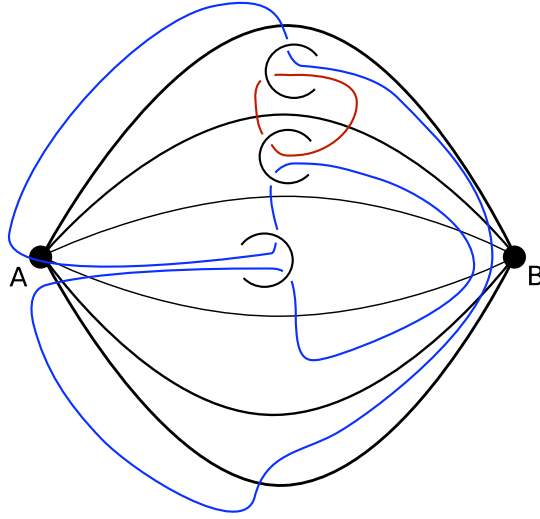


Figure 17: The corridor complex link for the face pairing from Section 3

complex link must have an unknotted edge component that wraps around exactly one face component, called an *earring*. Thus, we see that L cannot be a corridor complex link for $P(\epsilon)$.

We can resolve this problem somewhat with Proposition 30, which gives us a way of going from certain pure braids to corridor complex links. As an added bonus, the proof tells us exactly how to construct the faceted 3-ball and face pairing associated with the corridor complex link. First, though, we need the powerful Moore's Theorem, taken from [1].

Theorem 28. *Let X be a Hausdorff space and f a surjection from \mathbf{S}^2 onto X . Then X is homeomorphic to \mathbf{S}^2 if and only if for all $x \in X$, both $\mathbf{S}^2 \setminus f^{-1}(x)$ and $f^{-1}(x)$ are nonempty and connected.*

Now we define the special type of pure braid we need.

Definition 29. *Let L be a closed pure braid, represented by full twists. Form \widehat{L} by changing all the overlaps in L into intersection points. We say L is a connected pure braid if \widehat{L} is connected.*

Finally, we can go from a connected pure braid to a corridor complex link.

Proposition 30. *Let L' be the closure of a pure braid such that L' is connected. Represent L' in terms of full twists and inverse full twists. Straighten each full twist from strand i to strand j and place an unknot encircling strands i through j in its place. If we then add an earring to each unknot, the resulting link L is a corridor complex link.*

Proof. First, recall that L' can be represented as a closure of a product of full twists and

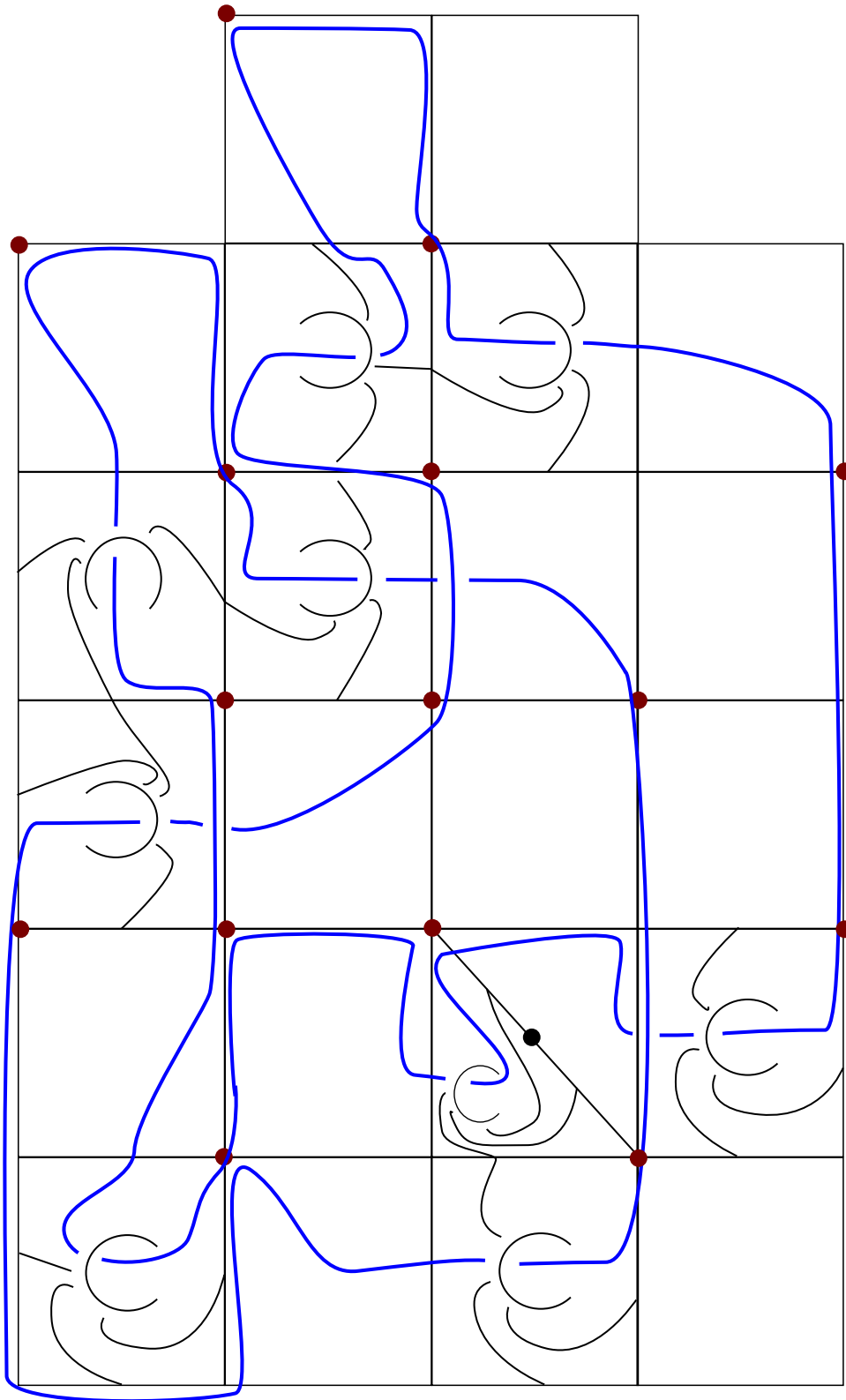


Figure 18: A partially drawn corridor complex link with a knotted edge component.

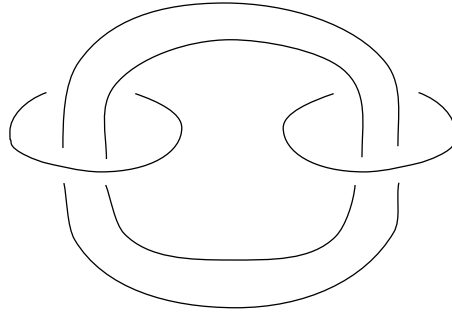


Figure 19: A link that looks like a corridor complex link, but is not.

inverse full twists by Proposition 11. Construct L from L' as instructed, and place the planar diagram for L in \mathbf{S}^2 . We will call the unknots we added around the straightened full twists face components. To construct the faceted 3-ball and face pairing for which L is a corridor complex link, first split each face component into two disks, with one placed slightly above the other. Strands that passed through a given face component should now enter the boundary of the top disk, vanish, and exit through the boundary of the bottom disk. No two disks should be overlapping. Place the point at infinity of \mathbf{S}^2 so that it lies inside one of the disks. Call the diagram we have formed Q .

Now we fatten each strand to a quadrilateral by foliating outward with line segments. We must foliate so that our quadrilaterals are concave with respect to the standard metric on $\mathbb{R}^2 = \mathbf{S}^2 \setminus \{\infty\}$, and a quadrilateral intersects another rectangle or itself only at its corners. Call the subsets with nonempty interior between foliated quadrilaterals and disks “empty space.” We form a quotient space by first collapsing the closure of each area of empty space to a single point, which we call a vertex point. Note that the closure of an area of empty space will contain some line segments and some points on the boundaries of disks. We also collapse each line segment which we haven’t collapsed already to a single point, which we call an edge point. Call points on the interior of disks face points (we do not collapse them). Collapsing forms an equivalence relation, call it \sim .

Let $\pi : \mathbf{S}^2 \rightarrow \mathbf{S}^2 / \sim$ be the projection map from a point to its equivalence class. Then every point $p \in \mathbf{S}^2 / \sim$, $\pi^{-1}(p)$ is closed. Since we did not collapse points in the interior of disks, it is not hard to verify that \mathbf{S}^2 / \sim is Hausdorff.

Let $p \in \mathbf{S}^2 / \sim$. It is clear that $\mathbf{S}^2 \setminus \pi^{-1}(p)$ and $\pi^{-1}(p)$ are nonempty. If p is a face point, then $\pi^{-1}(p)$ is a single point and $\mathbf{S}^2 \setminus \pi^{-1}(p)$ is connected. Now let p be a vertex. Then $\mathbf{S}^2 \setminus \pi^{-1}(p)$ contains every other area of empty space, every fattened edge strand, and every disk. But since Q has a strand connecting every pair of disks and L' was a connected pure braid, the disks and fattened edge strands form one connected component. The boundary of any area of empty space always contains only line segments and points on the boundary of disks, so $\mathbf{S}^2 \setminus \pi^{-1}(p)$ is connected. If p is an edge point, then $\pi^{-1}(p)$ is a line segment and again $\mathbf{S}^2 \setminus \pi^{-1}(p)$ is connected. Therefore, by Moore’s Theorem \mathbf{S}^2 / \sim is a two sphere.

We now have a recipe for creating a faceted 3-ball P with face pairing ϵ . Each disk becomes a face, each rectangle collapses to become an edge, and empty space collapses to form vertices. Disks are paired by reflection over their common edge, which is represented by an earring. It only remains to be seen that L is in fact the corridor complex link for P . Pick a disk d , paired with d' . Assume without loss of generality that in Q , the disk d was above d' . Place a face component c in d . Since d is paired with d' by reflection over a common edge, edge components in d start from its edges, go through c , pass directly into d' , and go to the edges of d' . This corresponds in Q to the strands coming into the top of d , entering d , disappearing through empty space and d' , and coming out the bottom of d' respectively. By reversing the construction of Q , we see that L must be the corridor complex link for P . \square

4.2 Statement of Key Theorems

Currently, the usefulness of bitwisted face pairings hinges on four theorems proved in [5]. Here I will summarize these results, and provide some insight as to their importance.

Theorem 31. *Let P be a cell structure on \mathbf{B}^3 , let ϵ be a face pairing on P , and let $m = (m_1, m_2, \dots, m_n)$ be a set of multipliers, one for each edge cycle of ϵ . Then $M = P(\epsilon, m)$ is a closed, connected, orientable 3-manifold.*

Theorem 32. *Let $M = P(\epsilon, m)$ be a bitwist manifold, and let L be the corridor complex link for $P(\epsilon)$. Give the face components of L framing 0. Give each edge component e of L framing $\frac{1}{\text{mul}([e])}$ plus the blackboard framing of the edge component, where $[e]$ is the edge cycle associated with e . Then Dehn Surgery on L with this framing will give M .*

Theorem 33. *Let L be a framed corridor complex link such that each face component has framing 0 and each edge component is framed by a rational number. Then Dehn Surgery on L with this framing will give a bitwist manifold.*

Theorem 34. *Every closed, connected, orientable 3-manifold is a bitwist manifold.*

Theorems 31 and 34 tell us that the bitwist construction always works, and that we can find a bitwist representation for every closed, connected, orientable 3-manifold. As we will see, the proof of Theorem 34 is constructive and will allow us to go from a surgery representation to a bitwist representation. Theorem 32 allows us to get a surgery representation from a bitwist representation. Along with Theorem 34 and twist moves, it provides a starting point for showing when two bitwist representations give the same manifold. Finally, Theorem 33 is essential to the proof of Theorem 34.

In the next two subsections I will prove Theorems 31 and 34. For Theorem 33, I will provide an example which should make the method of proof obvious. Although Theorem 33 is

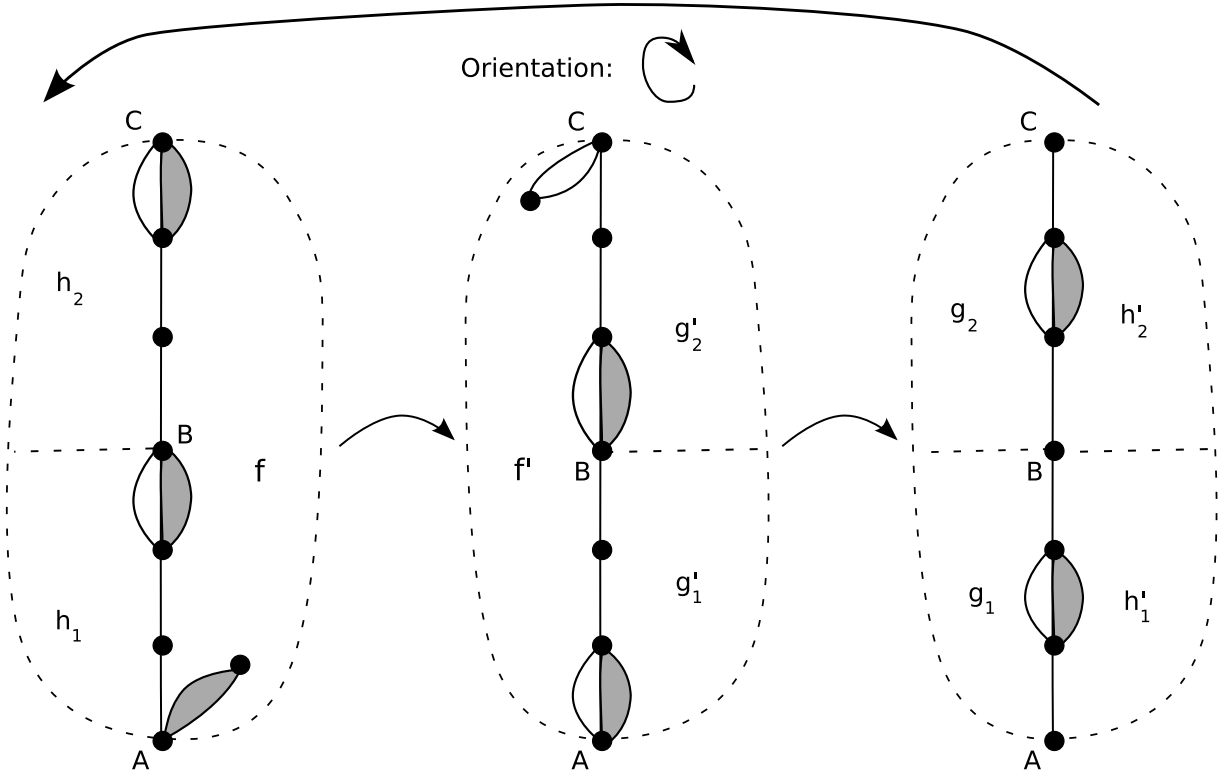


Figure 20: Diagram representing the edge cycle $[e]$. Shaded bubbles represent which face we pass through. The multipliers of AB and BC are both $+1$.

absolutely essential to the theory of bitwist manifolds, proving it requires the construction of Heegaard Diagrams for bitwisted face pairings and is beyond our scope. It is proved in full in [5].

4.3 Proof of the Construction

I will prove Theorem 31, that the bitwist construction always yields a manifold, by showing combinatorially that the resulting face pairing always has Euler Characteristic 0.

Proof. Let $Q(\delta)$ be obtained from $P(\epsilon)$ by subdividing original edges, adding stickers, and twisting ϵ as described in Section 3. If M is in fact a manifold, then we know it is connected, closed, and orientable because it is represented by an orientation reversing face pairing δ on the faceted 3-ball Q , so we need only show that $\chi(M) = c_0 - c_1 + c_2 - c_3 = 0$. Since M is a face pairing on \mathbf{B}^3 , the only 3-cell is \mathbf{B}^3 itself and so $c_3 = 1$. Likewise, if m is the number of faces of P as a faceted 3-ball, then $c_2 = m/2$.

Now I will show that due to twisting, $c_1 = c_2$. Pick a face f of Q , and let $E_1(n_1, j_1)$ be an original edge of f which is part of an edge cycle $[E_1]$ in ϵ with length n_1 and multiplier j_1 .

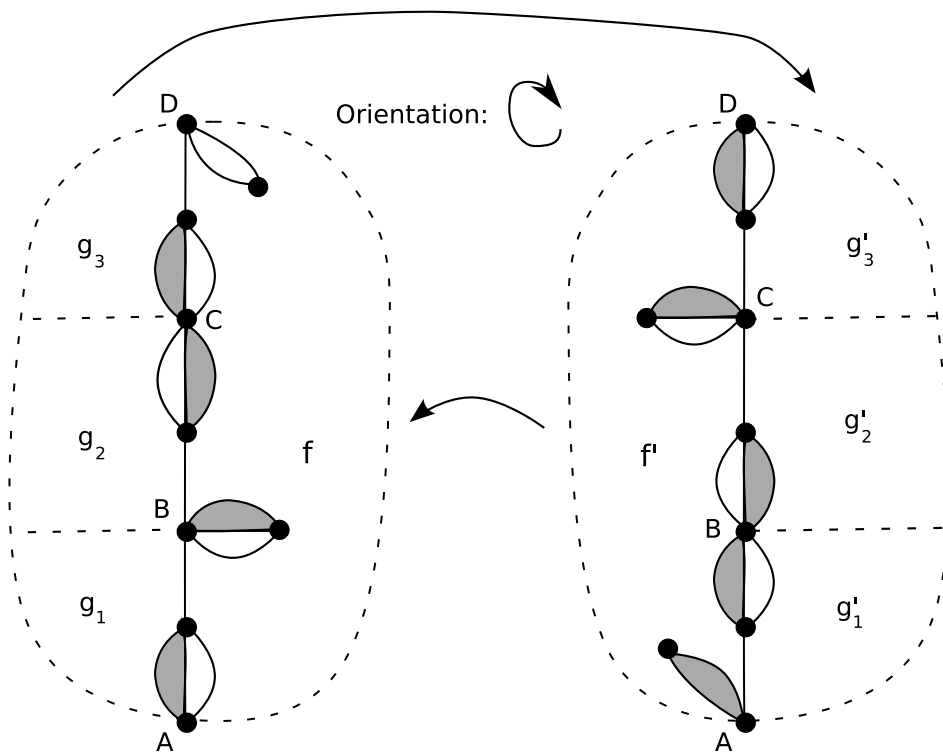


Figure 21: Diagram showing another edge cycle. The multipliers of AB , BC , and CD are -1 , 1 , and -1 respectively.

Let e be an edge which precedes E_1 in δ , by which we mean e is mapped onto one of the subedges in E_1 by δ and should be chosen as follows. Look at the original edge E_0 which precedes E_1 in the orientation. If $j_1 < 0$, then e is a subedge or sticker in f' which precedes $\epsilon(E_1)$ in orientation of f' . If $j_1 > 0$, then e is a subedge or sticker in f which precedes E_1 in orientation of f .

We now examine the edge cycle of e . Refer to Figures 20 and 21 to make the following analysis more clear. Because of twisting, the edge cycle $[e]$ moves through new edges of $[E_1]$ in the direction of orientation of f . In exactly $n_1 * |j_1|$ steps, e will have been carried to e' , which is either the preceding edge of E_2 (the next original edge in direction of orientation) or will be mapped to a sticker in the next step which is a preceding edge of E_2 . In this way, we see that $[e]$ contains one new edge for every new edge in ∂f . Because e always travels to preceding edges in f or f' , it is clear that we can find $m/2$ edge cycles, at least one for each pair of faces in Q . Since each edge is shared by exactly two faces, this means that these edge cycles contain every new edge. There cannot be an edge cycle that contains only stickers, since a sticker always precedes some original edge, and so these are the only edge cycles that can exist. Thus we have shown that $m/2 = c_2 = c_1$.

To see that $c_0 = 1$, notice that the edge cycles as described above take original vertices to adjacent original vertices. Since the 1-skeleton of Q is connected and every new vertex is taken to an original vertex, this shows that every vertex is equivalent and $c_0 = 1$.

To conclude, we have $\chi(M) = 1 - c_1 + c_1 - 1 = 0$, and by Theorem 26 M is a manifold. \square

4.4 Changing Edge Cycle Framings

In this section I will provide an example of how Theorem 33 can be applied in practice. I will also discuss what is involved in the proof of the theorem. For a complete discussion, see [5].

Let L be a corridor complex link. Let the face components of L have framing 0, and let the edge components of L be framed by arbitrary rational numbers. For our example, say some edge component e of L has framing $2/7$. We will change the framing of e to the reciprocal of an integer by adding a chain of linked unknots. The first unknot we add will be a face component around L , the next will be an edge component, the next a face component, etc. When we are done, we will know that Dehn Surgery on L gives a bitwist 3-manifold by Theorem 32.

Begin by adding a face component a_1 with framing $7/5$ around e through an inverse slam dunk. This changes the framing of e to 1, which is the reciprocal of an integer as required. Now we want a_1 to have integer framing, so that we can change its framing to 0 later. We get this by adding to a_1 an unknotted edge component a_2 with framing $5/3$ by an inverse slam dunk. This changes the framing of a_1 to 2. We like edge components to have framings which are reciprocals of integers, so we need to now change the framing of a_2 . Once again, we add

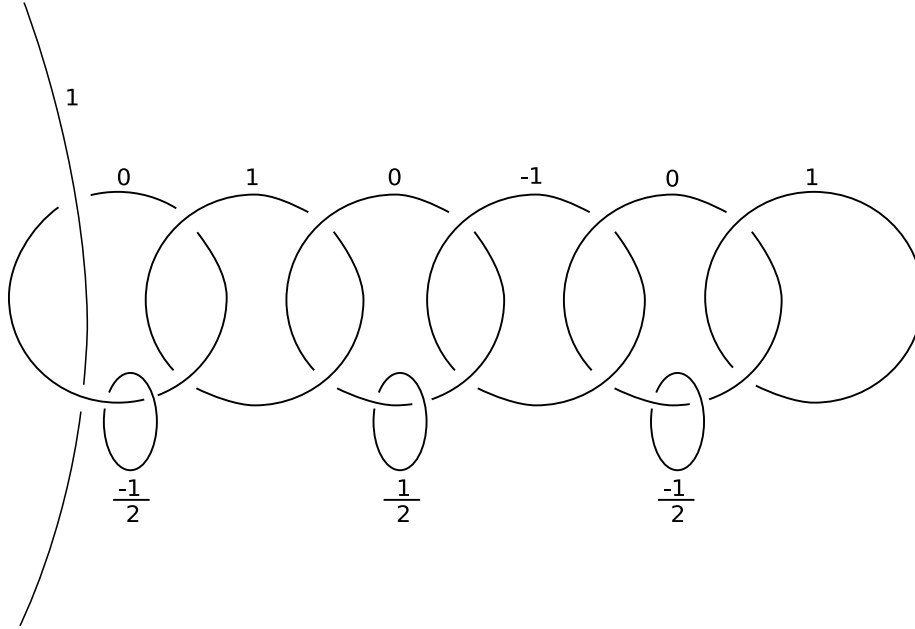


Figure 22: Adding alternating face and edge components to change the framing of an edge component from $2/7$ to 1 .

a face component through an inverse slam dunk. We must continue this process until we get a chain of alternating face and edge components that ends on an edge component with framing the inverse of an integer. In this particular case, we get six unknots with framings $a_1 = 2$, $a_2 = 1$, $a_3 = -2$, $a_4 = -1$, $a_5 = 2$, and $a_6 = 1$. Here we denote the framing of unknot a_n by a_n as well.

Now we will change the framings of the face components to 0 , and in doing so guarantee that L with the chain of unknots attached is a corridor complex link. To each unknot a_n with n odd, add an earring with framing ∞ . Then perform a twist of $-a_n$ revolutions on the earring. This changes the framing of the earring to $\frac{1}{-a_n}$ and the framing a_n to 0 . By Proposition 30 we have a corridor complex link for a face pairing $P(\epsilon)$, and by Theorem 32 we can pick multipliers so that the manifold obtained by Dehn Surgery on L gives the same manifold as $P(\epsilon, m)$.

If we successively destroy the unknots by slam dunks, we find that the original framing of e

is given by a simple continued fraction:

$$\frac{2}{7} = 1 - \frac{1}{2 - \frac{1}{1 - \frac{1}{-2 - \frac{1}{-1 - \frac{1}{2 - \frac{1}{1}}}}}}$$

Proving Theorem 33 comes down to proving that every rational number has a continued fraction representation of this type.

4.5 Proof of Main Result

Proving that every closed, connected, orientable manifold is a bitwist manifold (Theorem 34) is not difficult given the above results.

Proof. Let M be any closed, connected, orientable 3-manifold. By corollaries to the Dehn-Lickorish Theorem, M can be obtained by Dehn Surgery on a framed link L . By Proposition 10, L can be expressed as the closure of a pure braid. Then by Proposition 11, L can be expressed entirely by the closure of the product of full twists and inverse full twists.

For each full twist in L , add an unknot with framing ∞ which encircles it. Perform a one revolution twist in the positive direction on the unknot, which changes the framing of the unknot to $\frac{1}{1 + \frac{1}{\infty}} = 1$ and removes the full twist. Now add an earring with framing ∞ to the unknot, and perform a twist on it in the negative direction. This changes the framing of the earring to -1 , while changing the framing of the unknot to 0. During these steps, the framing of the pure braid strands (edge components) may change as well. We go through a similar process for each inverse full twist in L , except that the twist directions are reversed. Thus to undo an inverse full twist we end with an unknot with framing 0 and an earring with framing 1.

Now, by Proposition 30, we have constructed a framed corridor complex link and each face component has framing 0. Thus, by Theorem 33, we can through twist moves alter the framings of the edge components so that they are all reciprocals of integers and we still have a corridor complex link. Finally, by Theorem 32, the face pairing with appropriate multipliers corresponding to our corridor complex link is the bitwist representation for M . \square

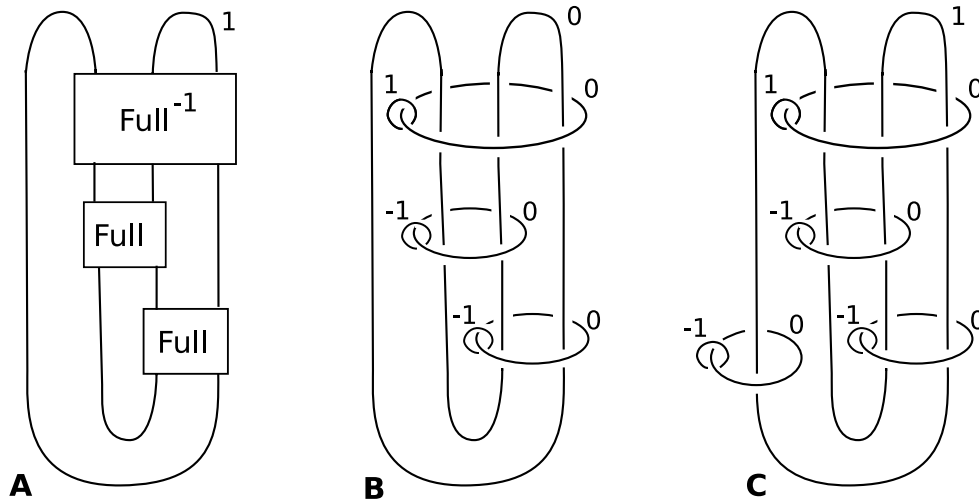


Figure 23: A: The trefoil knot represented by full twists with framing 1. B: A corridor complex link obtained from A. C: Changing the framing of an edge component so that the new framing is the reciprocal of an integer.

5 Applications of Results to 3-Manifold Construction

In this section, I will show how to apply the results from above to generate bitwist representations of common 3-manifolds.

5.1 The Poincaré Sphere

The Poincaré Sphere was the first example of a topological space with the homology of the 3-sphere, but without having trivial fundamental group. Poincaré constructed it himself as a counterexample to what he had first conjectured, that any manifold with the same homology as a sphere was homeomorphic to a sphere. His discovery of what became known as the Poincaré Sphere proved his first conjecture to be false, leading him to the now famous Poincaré Conjecture (which has turned out to be true). Using a surgery representation, corridor complex links, and Theorem 34 we will construct a bitwist representation of this important manifold.

We start by noting that Dehn Surgery on the trefoil with framing 1 yields the Poincaré Sphere, see [10] page 110. To use the construction given in the proof of Theorem 34, we start by finding a pure braid representation of the trefoil, which we have already done in Figure 2. Following Proposition 11, we get the full twist representation given in Figure 23 A.

Now we need to use twist moves to obtain a corridor complex link. First we add three unknots with framing ∞ around each of the full twists. On the unknot that wraps around

the inverse full twist on three strands, we perform a twist in the negative direction. This undoes the inverse full twist, and changes the framing of the braid to $1 - \text{lk}^2(K, J) = 0$, where K is the unknot and J is the braid. The framing of the unknot becomes $\frac{1}{-1 + \frac{1}{\infty}} = -1$. To be a properly framed face component, the unknot needs framing 0. To get this, we add an earring with framing ∞ to the unknot and do a positive twist on the earring. This changes its framing to 1, while changing the framing of the unknot to 0.

On each unknot that wraps around a full twist on two strands, we do a positive twist. This undoes the positive full twists, and changes the framing of the unknot to 1. The framing of the braid remains 0, since $\text{lk}(K, J) = 0$ in both cases. As before, we change the framings of the unknots to 0 by adding earrings with framing ∞ , but we do a negative twist on each earring so that they both have framing -1 and the unknots have framing 0.

At this point, we have the framed corridor complex link shown in Figure 23 B. However, we cannot easily find a bitwist description for the Poincaré Sphere using this corridor complex link because one of the edge components has framing 0. Our goal is to change that framing to the reciprocal of an integer, so that we can use Theorem 32.

Add an unknot with framing ∞ so that it wraps around a single strand of the edge component with framing 0. Then $\text{lk}^2(K, J) = 1$. Doing a positive twist on the unknot changes the framing of the edge component to $0 + 1 = 1$, and the framing of the unknot to 1. Now add an earring to the unknot with framing ∞ , and do a negative twist on the earring so that its framing changes to -1 . The framing of the unknot becomes 0, and we have the corridor complex link shown in Figure 23 C.

To obtain a face pairing from Figure 23 C, we follow the process described in the proof of Proposition 30. First, we pull through part of the braid edge component so that the quadrilateral face component becomes a digon face component. Then we split each face component into two disks, with the strands that pass through them disappearing as they enter the top disk but then coming back out of the bottom disk. The strands now partition the boundary of each disk up into edges and vertices. We get the diagram shown in Figure 24.

Each pair of disks represents two faces of a faceted 3-ball, paired by reflection. This induces a face pairing $\epsilon = (\epsilon_1, \epsilon_2, \epsilon_3, \epsilon_4)$.

$$\begin{aligned} \epsilon_1 : \begin{pmatrix} A & 1 & B & 2 \\ A & 3 & B & 2 \end{pmatrix} & \quad \epsilon_2 : \begin{pmatrix} A & 3 & B & 4 \\ A & 5 & B & 4 \end{pmatrix} & \quad \epsilon_3 : \begin{pmatrix} A & D & B & 5 \\ A & D & C & 1 \end{pmatrix} \\ & & \quad \epsilon_4 : \begin{pmatrix} C & B & 1 & D \\ C & B & 1 & A \end{pmatrix} \end{aligned}$$

The strands in Figure 24 tell us what edges are shared between faces. Starting with $T1$ and $T1'$ and working outwards, we get the faceted 3-ball P shown in Figure 25. The manifold $M = P(\epsilon, (1, 1, -1, -1, -1))$ is the Poincaré sphere, by Theorem 32.

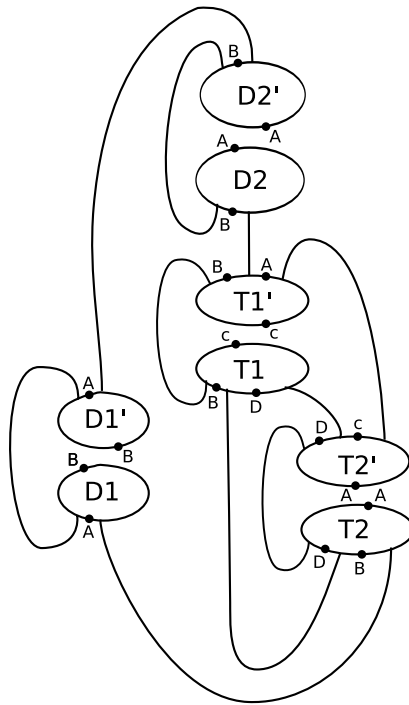


Figure 24: Applying Proposition 30 to the corridor complex link in Figure 23 C.

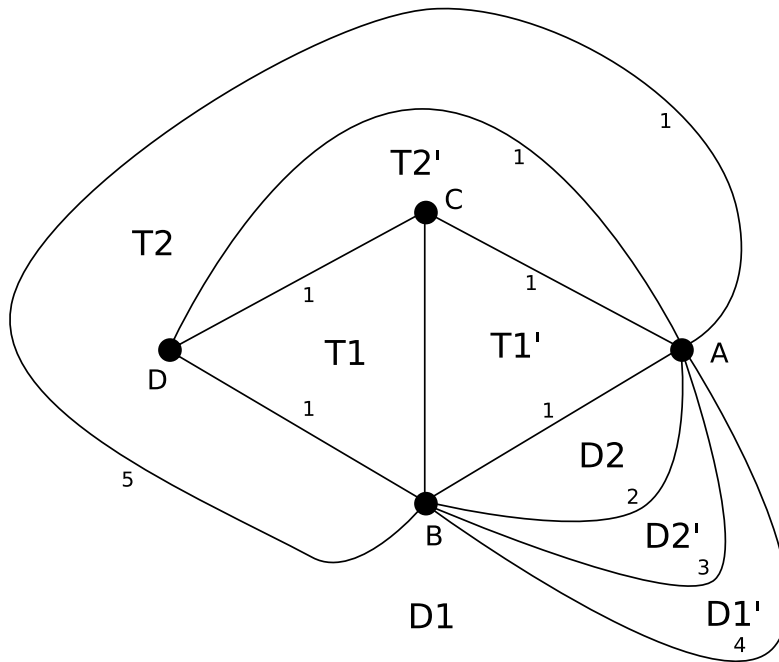


Figure 25: A faceted 3-ball described by Figure 24.

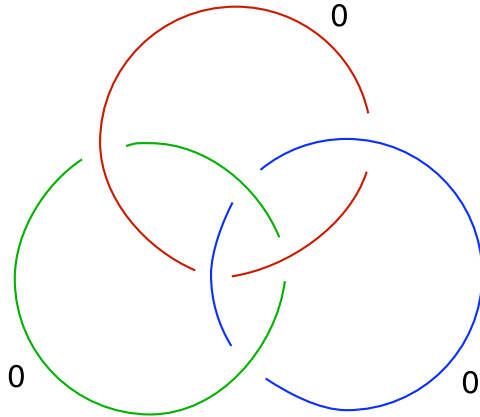


Figure 26: The Borromean Rings with framing 0

5.2 The 3-Torus

We will use a method similar to that which we used to obtain the Poincaré Sphere to obtain the 3-torus, \mathbb{T}^3 . We begin with the Borromean rings, shown in Figure 26. This link is particularly interesting because if any one of the three unknots is omitted, we can unlink the other two unknots. More important to us, though, is that Dehn Surgery on the Borromean Rings with framing 0 gives the 3-torus (see [7]).

Building the Borromean rings out of shoe strings, it is possible to find the pure braid representation shown in Figure 27 A. Using Proposition 11, we can represent the pure braid in terms of full twists, as shown in Figure 27 B.

Now we use the same process we used for the Poincaré Sphere above. To undo each full twist, we add an unknot with framing 1. To undo each inverse full twist, we add an unknot with framing -1 . We add earrings with framing -1 to unknots with framing 1, and earrings with framing 1 to unknots with framing -1 . This changes the framings of the unknots to 0. Examining linking numbers and twist directions, we find that the framing of two links in the pure braid remain unchanged and the framing of the last one is changed to 1. At this point we have the corridor complex link shown in Figure 28 A.

Just like when we constructed the Poincaré Sphere, we have run into the problem of having edge components with framing 0, which is not the reciprocal of any integer. We fix this by adding two additional unknots with framing ∞ , each around one of the strands of the link with framing 0. We give each added unknot a positive twist and then add earrings to them with framing -1 . This yields the corridor complex link shown in Figure 28 B.

Now we can use Proposition 30 to obtain the diagram shown in Figure 29. This figure describes a faceted 3-ball shown in Figure 30, with faces paired by reflection. We can choose multipliers by looking at the framings of edge components in the corridor complex link.

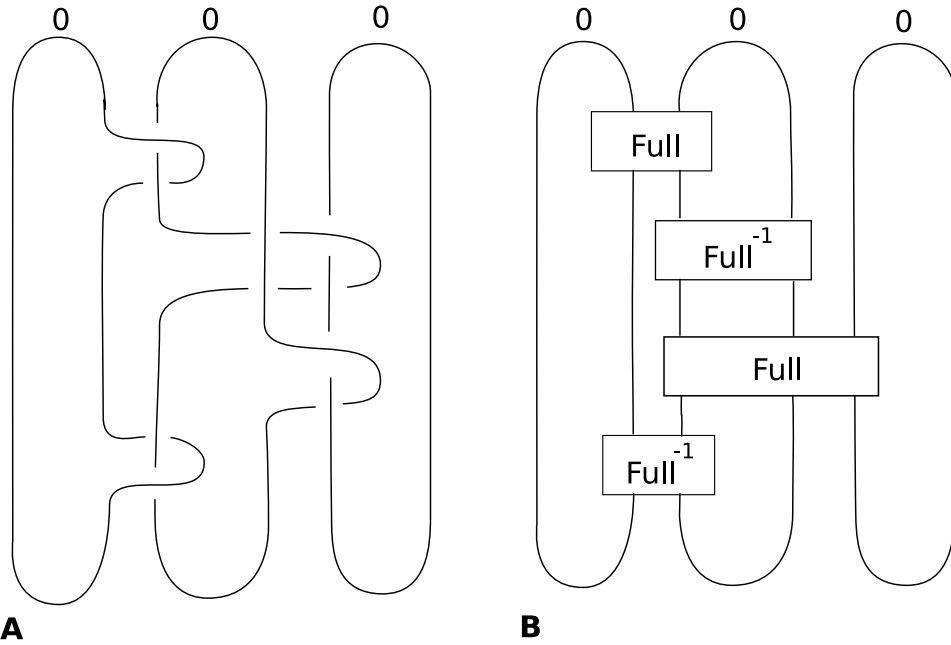


Figure 27: A: The Borromean Rings with framing 0 as the closure of a pure braids. B: The full twist representation of A

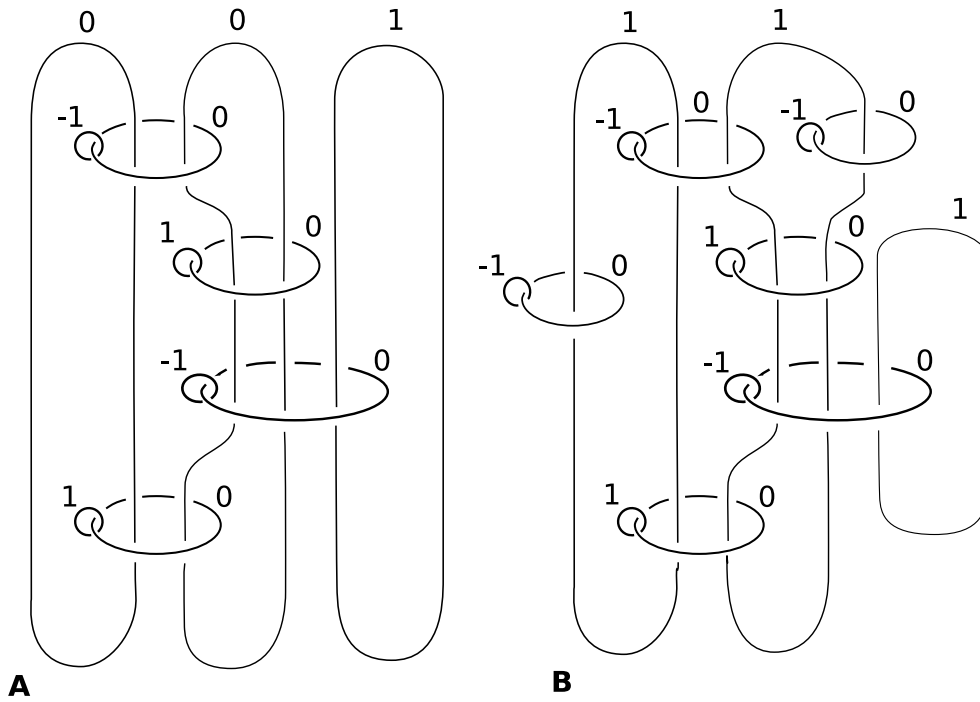


Figure 28: A: A corridor complex link obtained from Figure 27. B: A altered so that every framing is the inverse of an integer.

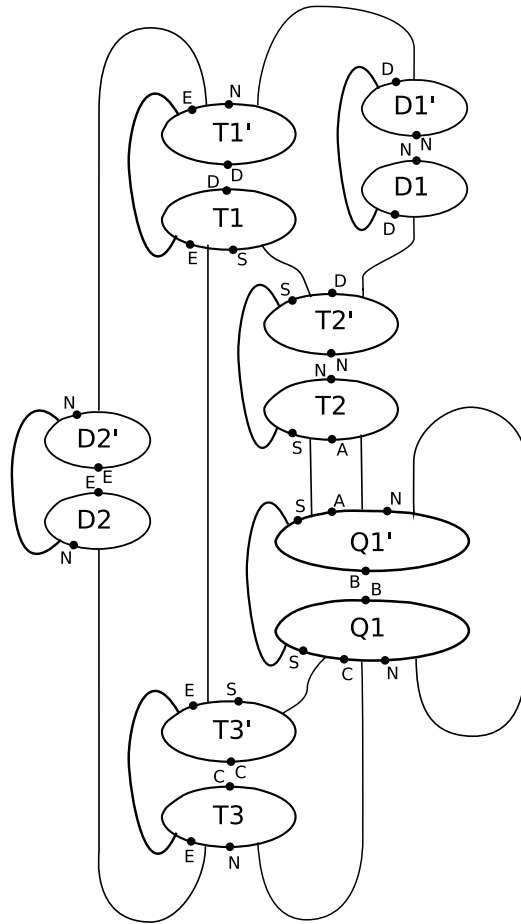


Figure 29: Applying Proposition 30 to the corridor complex link in Figure 28 B.

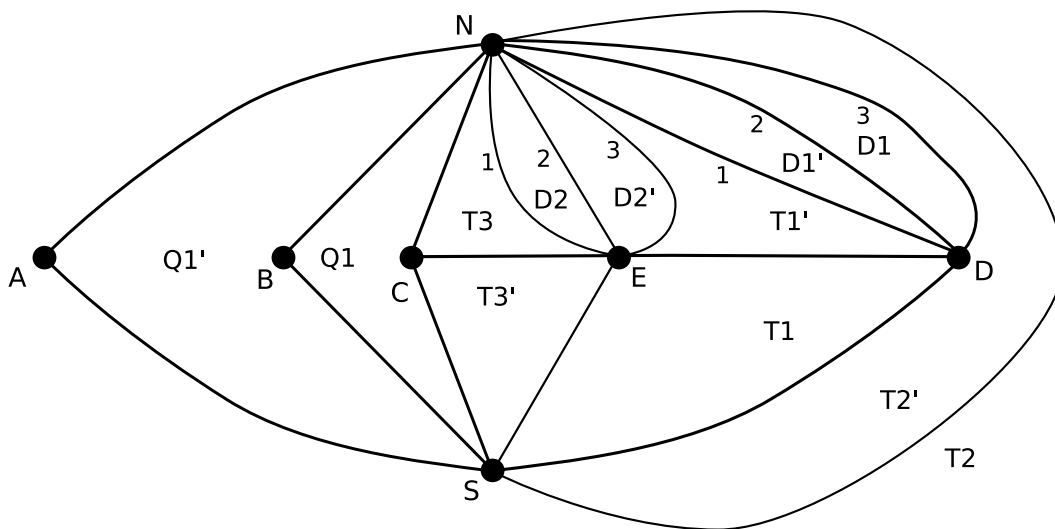


Figure 30: A faceted 3-ball obtained from Figure 29.

6 Equivalence of Bitwist Representations

Using twist moves, we can tell whether two surgery representations give homeomorphic manifolds. A natural question to ask is whether a set of operations exists which will tell us if two bitwist representations give homeomorphic manifolds. As yet this question is unanswered, but as we will see the relationship between bitwist representations and surgery representations gives us a starting point. First, though, we state the following result from [5].

Theorem 35. *Let P be a faceted 3-ball, ϵ a face pairing on P , and $m = (m_1, m_2, \dots)$ a set of multipliers for ϵ . Then $P(\epsilon, m)$ is homeomorphic to $P(\epsilon, -m)$.*

This says that reversing the twist direction of every edge leaves the topology of the resulting manifold unchanged.

For the next few subsections, we need to know how to destroy an unknot in a framed link diagram. Let L be the planar diagram of a link, and let c be an unknot with framing $r \in \mathbb{Z}$. Do a twist by $-r$ revolutions on c to obtain the framed link L' . Then the framing of c changes to $r' = \frac{1}{-r+r} = \infty$. Now, the framing ∞ describes a curve $\gamma = \alpha$, which is just a meridian. Then Dehn Surgery on c is the identical surgery, and we can remove c from L' .

6.1 Equivalence of 3-Torus Representations

Recall that in Section 3 we calculated that the corridor complex link of our bitwist manifold M was $\mathbb{Z} \times \mathbb{Z} \times \mathbb{Z} = \pi_1(\mathbb{T}^3)$. By using twist moves on the framed corridor complex link for M , we can prove that M is in fact the 3-torus.

Figure 31 A shows a link equivalent to the corridor complex link for M , which we calculated earlier in Figure 17. We frame the link as instructed by Theorem 32, so that the edge components have framings equal to the inverses of the multipliers of their corresponding edge cycles. We start by destroying the edge component with framing 1, by performing a negative twist on it. This links the two face components with framing 0 which pass through it, and changes both their framings to -1 (Figure 31 B). We now can destroy one of the two face components by doing a positive twist on it. This links the remaining face component with the remaining edge component, and gives every link component framing 0. We now have the link in Figure 31 C, which is equivalent to the Borromean Rings with framing 0. Thus, by Theorem 32, M is the 3-torus.

Notice that we now have two representations for the 3-torus. One was discovered systematically by turning the Borromean Rings into a pure braid. The one discussed above was actually discovered by mistake. We can get one more representation for the 3-torus by noticing that the link in Figure 31 looks like it might be a corridor complex link already. There

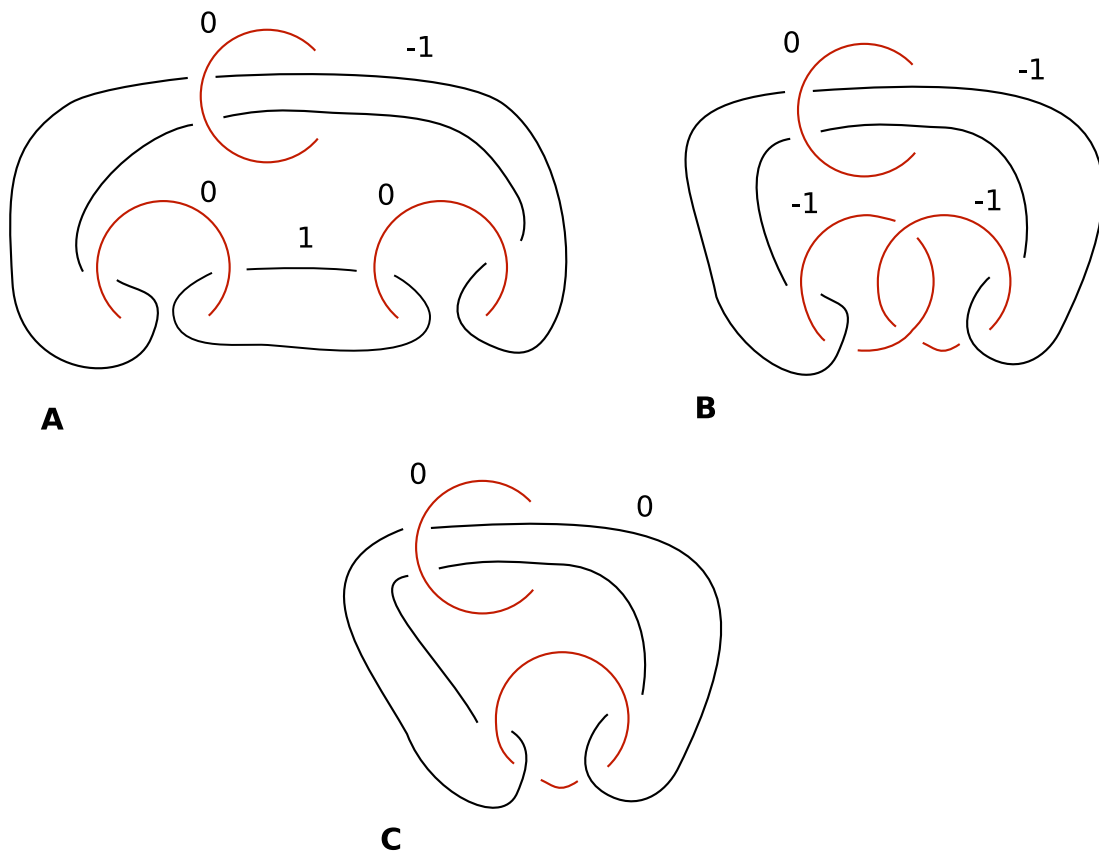


Figure 31: Using twist moves to go from the corridor complex link for the bitwist manifold constructed in Section 3 to the Borromean Rings with framing 0.

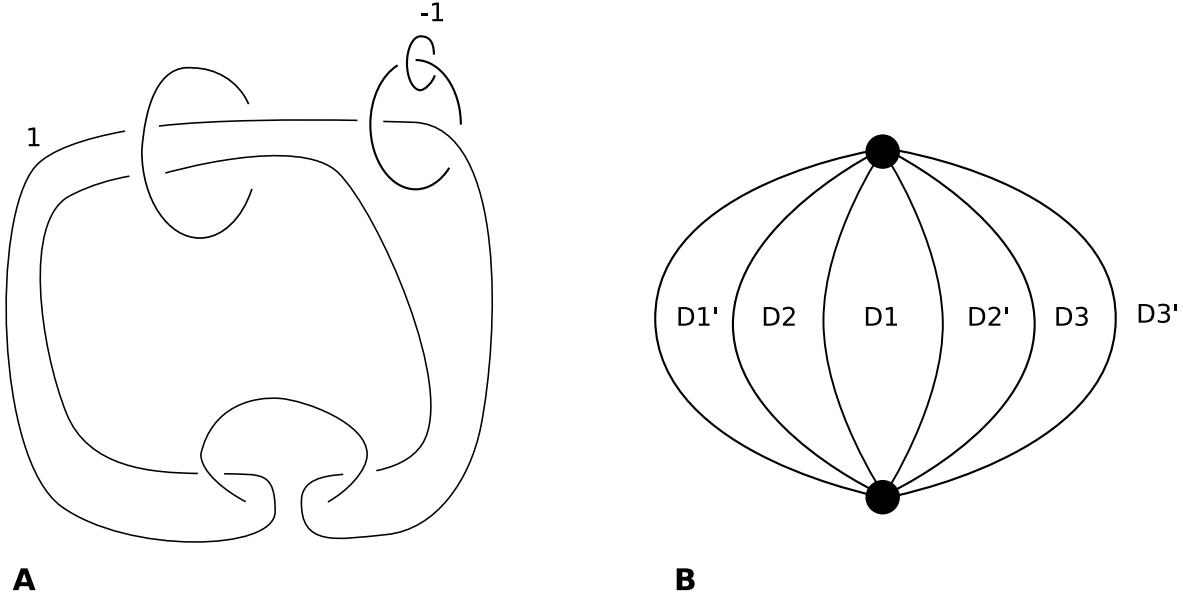


Figure 32: A: The corridor complex link for our third representation of the torus. B: Face pairing with the corridor complex link shown in A. Faces are paired by reflection.

are two face components, both with framing 0. To apply Theorem 32, we need merely to change the framing of the one edge cycle and hope we have a corridor complex link. We can do this as we've done before, by adding an unknot with earring around one of the strands of the edge cycle. As shown in Figure 32 A, the new unknot will have framing 0, the earring framing -1 , and the edge cycle framing 1. The process outlined by Proposition 30 works for the resulting link, and results in a third representation for the 3-torus. The face pairing for this new representation is shown in Figure 32 B.

It's also worth noting at this time that the Borromean Rings are a corridor complex link in their own right. One can verify this through the standard process.

6.2 Equivalence of Poincaré Sphere Representations

We begin this section by noting that the Poincaré Sphere can be obtained by Dehn Surgery on the Borromean Rings with framing 1. Using twist moves, one can go from the trefoil with framing 1 to the Whitehead Link to the Borromean Rings with framing 1 (see [10]). If we follow the same process we did for construction the 3-torus in Section 5.2, we get a faceted three ball that looks almost exactly the same as the one in Figure 30, except the two digons are gone.

We can get a third representation for the Poincaré Sphere by modifying the Borromean Rings directly. Considering the Borromean Rings with framing 1 as a corridor complex link, we add an earring with framing -1 to each face component. The result, shown in Figure 33

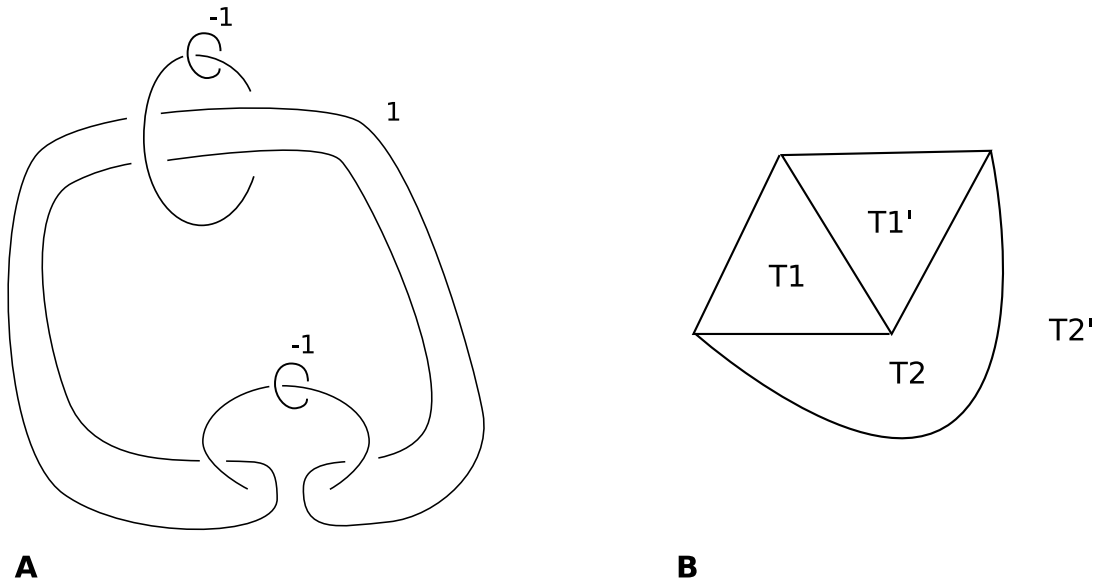


Figure 33: A: Corridor complex link for a new representation of the Poincaré Sphere. B: Faceted 3-ball with face pairing for A. Faces are paired by reflection over their common edges.

A, is clearly a corridor complex link and by following the Proposition 30 process we get the face pairing shown in Figure 33 B.

Notice that this representation is very similar to the representation in Figure 25, except that four faces have been collapsed. Looking at Figure 23 C, it is not hard to see why. If we pull the last two strands of the pure braid through the triangle face component, we get two digon face components. One has an earring with framing 1 , and the other has an earring with framing -1 . We first destroy each earring through a twist move, and then destroy each unknot with a twist move. This process leaves the framing of the big edge component unchanged, leaving us with the corridor complex link in Figure 33 A. Using twist moves to remove two face components, we effectively collapsed four faces.

6.3 Changing Multipliers

In this section we discuss multipliers, and show that in some cases they can be changed without changing the resulting manifold. First, notice that multipliers other than 1 and -1 are not actually necessary at all. If m is a multiplier for an edge cycle $[e]$ and $|m| > 1$, we can change m to 1 or -1 by subdividing each edge in $[e]$ into $|m|$ edges. The reason multipliers are used is to simplify the faceted 3-balls used as input to the bitwist construction, and to get results about families of examples.

To see that changing multipliers does not always change the topology of a bitwist manifold,

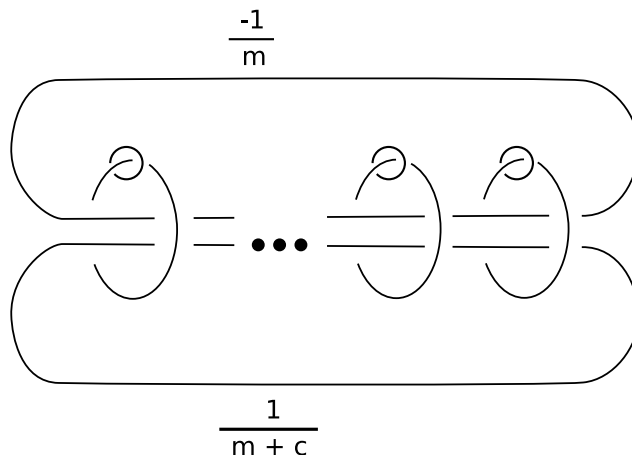


Figure 34: A framed corridor complex link L .

consider the link L shown in Figure 34. L is a corridor complex link for some face pairing $P(\epsilon)$ by Proposition 30. Let $c \in \mathbb{Z}$ be fixed and $m \in \mathbb{Z} \setminus \{0\}$ be arbitrary such that $m+c \neq 0$. Then using twist moves we can always eliminate both of the non-earring edge components, which adds c full twists to the strands of the face components passing through the bottom edge component, and change the framings of the former face components to $-c$. Thus the manifold obtained by Dehn Surgery on L is independent of m . But by Theorem 32, the framings of edge components correspond to multipliers assigned to edge cycles in $P(\epsilon)$. Since the manifold obtained by Dehn Surgery is the same for any choice of m , so is the manifold obtained by the bitwist construction for any choice of m when assigning multipliers.

7 Further Research

Though in this paper we have found some equivalent bitwist representations, there is yet no general method for doing this. Ideally, we would like something similar to twist moves except for bitwist representations rather than framed links.

In Section 6, I've shown how one might try to find such a set of moves by analyzing corridor complex links. Perhaps the biggest obstacle to developing such a set of moves, then, is that we don't know when a given link is a corridor complex link. The corridor complex links we've used throughout this paper have been relatively tame as knots go, but far more complicated corridor complex links are possible (see for example, Figure 18). With this in mind, I pose the following questions:

1. Which links are corridor complex links?
2. What sequences of twist moves takes a corridor complex link to another corridor complex link?

3. When does a face pairing have a corridor complex link with knotted edge components?

There are several other interesting, open questions related to the construction and application of bitwist manifolds. Finding answers to any of these questions would make the bitwist construction more useful to the study of low dimensional topology.

1. Is there an algorithm to go from an arbitrarily expressed pure braid to an equivalent pure braid expressed as the product of generators?
2. In what ways does changing the multipliers affect the topology of the manifold obtained by the bitwist construction? What about the geometry of the manifold?

Bibliography

- [1] J. W. Cannon and G. R. Conner, *The homotopy dimension of codiscrete subsets of the 2-sphere \mathbf{S}^2* , *Fund. Math.* **197** (2007), 35–66.
- [2] J. W. Cannon, W. J. Floyd, and W. R. Parry, *Introduction to twisted face-pairings*, *Math. Res. Lett.* **7** (2000), 477–491.
- [3] J. W. Cannon, W. J. Floyd, and W. R. Parry, *Twisted face-pairing 3-manifolds*, *Trans. Amer. Math. Soc.* **354** (2002), 2369–2397.
- [4] J. W. Cannon, W. J. Floyd, and W. R. Parry, *Heegaard diagrams and surgery descriptions for twisted face-pairing 3-manifolds*, *Algebr. Geom. Topol.* **3** (2003), 234–285 (electronic).
- [5] J. W. Cannon, W. J. Floyd, and W. R. Parry, *Bitwist 3-manifolds*
- [6] N. M. Dunfield, W. P. Thurston, *Finite Covers of Random 3-manifolds*, *Invent. Math.* **166** (2006) 457–521.
- [7] R. E. Gompf and A. I. Stipsicz, *4-Manifolds and Kirby Calculus*, Graduate Studies in Math., Vol. 20, Amer. Math. Soc., Providence, 1999.
- [8] K. Jänich, S. Levy, trans. *Topology*, Springer-Verlag New York Inc, 1984
- [9] A. Kawauchi, *A Survey of Knot Theory*, Birkhäuser Verlag, Basel-Boston-Berlin, 1996.
- [10] V. V. Prasolov and A. B. Sossinsky, *Knots, Links, Braids and 3-Manifolds*, Amer. Math. Soc., Providence, 1997.
- [11] W. P. Thurston, *Three-Dimensional Geometry and Topology*, Vol. 1, Princeton University Press, Princeton, 1997.
- [12] J. Weeks, *SnapPea: A computer program for creating and studying hyperbolic 3-manifolds*, available by anonymous ftp from geom.umn.edu/pub/software/snappea/.